

# UC San Diego

## UC San Diego Electronic Theses and Dissertations

### Title

Investigating the Role of the Adult Maize Leaf Cuticle in Providing Pathogen Resistance

### Permalink

<https://escholarship.org/uc/item/192111d7>

### Author

Nguyen, Albert Minh Tri

### Publication Date

2019

Peer reviewed|Thesis/dissertation

UNIVERSITY OF CALIFORNIA SAN DIEGO

Investigating the Role of the Adult Maize Leaf Cuticle in Providing Pathogen Resistance

A Thesis submitted in partial satisfaction of the requirements  
for the degree Master of Science

in

Biology

by

Albert Minh Tri Nguyen

Committee in charge:

Laurie Smith, Chair  
Alisa Huffaker  
Stanley Lo

2019

Copyright

Albert Minh Tri Nguyen, 2019

All rights reserved.

The Thesis of Albert Minh Tri Nguyen is approved, and it is acceptable in quality and form for publication on microfilm and electronically:

---

---

---

Chair

University of California San Diego

2019

## DEDICATION

I dedicate my work to my family and to the advancement of our scientific community.

## EPIGRAPH

...

I doubted if I should ever come back.

I shall be telling this with a sigh  
Somewhere ages and ages hence:  
Two roads diverged in a wood, and I—  
I took the one less traveled by,  
And that has made all the difference.

The Road Not Taken, by Robert Frost

## TABLE OF CONTENTS

Signature Page .....	iii
Dedication .....	iv
Epigraph .....	v
Table of Contents .....	vi
List of Figures .....	vii
List of Tables .....	viii
Acknowledgements .....	ix
Abstract of the Thesis .....	x
Chapter 1: Introduction .....	1
Chapter 2: Materials and Methods .....	21
Chapter 3: Results .....	26
Chapter 4: Discussion .....	45
Chapter 5: References .....	52

## LIST OF FIGURES

Figure 1.1. Plant cuticle structure and wax composition .....	4
Figure 1.2. Cutin chemical components and structure.....	5
Figure 1.3. Cutin and cuticle wax biosynthesis pathways .....	6
Figure 1.4. General wax classes commonly found in maize cuticle and their structures .....	7
Figure 1.5. Morphological example of a <i>glossy</i> mutant seedling’s distinguishable phenotype .....	8
Figure 1.6. Tissue-specific RNA expression profile for known <i>glossy</i> genes in inbred B73 .....	11
Figure 1.7. Agricultural symptoms and life cycle of <i>C. heterostrophus</i> .....	16
Figure 1.8. <i>C. heterostrophus</i> infection on maize leaf surfaces.....	17
Figure 1.9. Maize infected with <i>C. graminicola</i> .....	19
Figure 1.10. <i>C. graminicola</i> infection process.....	19
Figure 3.1. Adult-stage W22 and <i>glossy</i> mutants grown under greenhouse conditions .....	27
Figure 3.2. Juvenile wild-type W22 leaves infected with <i>C. heterostrophus</i> .....	28
Figure 3.3. Visual disease progression of W22 and <i>glossy</i> mutant detached leaves infected with <i>C. heterostrophus</i> .....	28
Figure 3.4. GFP quantification of GFP- <i>C. heterostrophus</i> droplet infection sites .....	29
Figure 3.5. <i>C. heterostrophus</i> droplet infection site on maize leaf tissue visualized for adhesion assay quantification.....	31
Figure 3.6. <i>C. heterostrophus</i> conidia adherence rates to W22 and <i>glossy</i> mutant leaf surfaces ..	32
Figure 3.7. Visual disease progression of W22 and <i>glossy</i> mutant detached leaves infected with <i>C. graminicola</i> .....	34
Figure 3.8. Quantification of GFP- <i>C. graminicola</i> droplet infection sites .....	38
Figure 3.9. <i>C. graminicola</i> droplet infection site on maize leaf tissue visualized for adhesion assay quantification.....	37
Figure 3.10. <i>C. graminicola</i> conidia adherence rates to W22 and <i>glossy</i> mutant leaf surfaces ....	38
Figure 3.11. Overall total cuticle wax load and wax classes of W22 and <i>glossy</i> mutants.....	41
Figure 3.12. Individual cuticle wax constituents organized by carbon chain length in adult wild-type W22 and <i>gl11</i> mutants .....	43
Figure 3.13. Individual cuticle wax constituents organized by carbon chain length in adult wild-type W22 and <i>gl17</i> mutants .....	44



## LIST OF TABLES

Table 1.1. Published cloned <i>glossy</i> mutants and their proposed gene functions .....	9
Table 2.1. <i>glossy</i> genotype panel allele and stock identities with introgression status into W22 background.....	21

## ACKNOWLEDGEMENTS

First, I would like to thank Dr. Laurie Smith and Dr. Susanne Matschi, my principal investigator and supervising post-doctoral researcher, who created an opportunity and accepted me as their student in the laboratory during a time in my academic career when I felt particularly lost. I was nearing the end of my undergraduate education, intimidated by the prospect of starting my career without work experience, and needed someone to give me a chance to prove my worth. Their continued support, guidance and dedication gave me direction and inspired me to continue in science.

I would also like to thank Miguel Vasquez, Hiep Ha, and other temporary members of the lab who supported me on infection days to help prevent the inevitable onset of pipet carpal tunnel in my right thumb and spent long nights in the microscope room with me. Additionally, I would like to thank Miguel, Kaiyue (Katy) Deng, Emily Kawabata and Dr. Paula Doblaz-Ibanez, who gave me constructive criticism on my research and later became life-long friends.

I would like to thank the BIMM 121 staff, team, and students for continuously funding my graduate studies at UCSD, being there for me during the difficult moments of research and inspiring me to pursue a career in science education.

We would like to thank some collaborators for their contributions to our study. We acknowledge Miguel Vasquez, who generated TEM photos of adult maize cuticle, and Dr. Isabel Molina and Dr. Richard Bourgault, collaborators from Algoma University, Canada, who generated the cuticle wax analysis. Subsequent maize cuticle wax extraction and GC/MS processing on the *glossy* genotype panel shown in this study was performed by Dr. Bourgault.

Lastly, I would like to thank my parents, my sister and friends for their support.

## ABSTRACT OF THE THESIS

Investigating the Role of the Adult Maize Leaf Cuticle in Providing Pathogen Resistance

by

Albert Minh Tri Nguyen

Master of Science in Biology

University of California San Diego, 2019

Professor Laurie G. Smith, Chair

The plant cuticle is a waxy, hydrophobic coating found on all aerial non-woody plant tissue and serves as a physical barrier protecting the plant from environmental stresses including pathogen infection, dehydration, and UV radiation. Studies on the plant cuticle in various plant model systems show differences in ultrastructure and chemical composition across different plant species, and even within a species, depending on many factors: organ identity, developmental stage and growth conditions. Little functional analysis has been performed to characterize the cuticle's relationship to pathogen resistance in adult *Zea mays*, thus leaving the agronomic impact of the cuticle on the adult-stage plant health largely unknown. Maize *glossy* mutants have defects in cuticle production—examples include lines with impaired levels of lipid biosynthesis or wax

transport proteins, making them effective tools to study the cuticle's impact on pathogen resistance.

In this study, we take a panel of *glossy* mutants and observe their differences in early stages of pathogen resistance to *Cochliobolus heterostrophus* and *Colletotrichum graminicola*, causal agents of Southern Leaf Blight and Anthracnose Stalk Rot, respectively. After establishing methods to observe and quantify GFP-labelled strains of these fungal infections on adult plants, which include fungal adhesion and long-term visual lesion formation, we detected differences in pathogenicity and cuticle wax profiles among our tested *glossy* mutants by utilizing epifluorescence microscopy, fungal quantification and gas chromatography/mass spectrophotometry. Combined with preliminary data on fungal penetration with confocal microscopy, these results will guide further investigation in elucidating the relationship between adult maize cuticle and pathogen resistance.

## CHAPTER 1: Introduction

Plant disease resistance mechanisms in agronomically important crops have been widely studied. According to the Food and Agriculture Organization of the United Nations (FAOSTAT) as of 2017, the United States is the world's leading producer of maize with about 371 million metric tonnes of maize produced (FAOSTAT 2018). Reductions in maize crop output due to disease has major, global agronomic implications. For example, during the 1970 North American agricultural year, Southern Corn Leaf Blight (SCLB) destroyed an estimated 15% of the total corn crop output, totaling an estimated loss of \$1.0 billion (adjusted to over \$6.0 billion in 2015 due to inflation; Ullstrup 1972, Bruns 2017). This epidemic prompted the agriculture industry to increase the genetic diversification of hybrid corn seed usage in subsequent seasons in the corn industry and sparked further research in maize resistance to SCLB. Ongoing research in plant defense against microbial pathogens has elucidated many genetic and biochemical bases for plant pathology, which include topics such as Pattern-Triggered Immunity (PTI), Effector-Triggered Immunity (ETI), Resistance (R) genes, plant breeding programs specific for hybrid-related immunity, and cuticle-pathogen relationships (Jones and Dangl 2006).

### **Plant immunity**

PTI, ETI and subsequent upregulation of biochemical signaling pathways are widely studied in plant immunity. Upon initial pathogen attack, plant pattern recognition receptors (PRRs) at the cell surface recognize widely conserved microbial- or pathogen-associated molecular patterns (MAMPs or PAMPs). Initial microbial damage can also trigger PRR recognition of damage-associated molecular patterns (DAMPs) (Boller and Felix 2009). Pathogen recognition results in rapid PTI response, which includes production of reactive oxygen species (ROS), salicylic acid (SA), a systemic acquired resistance (SAR) signaling molecule, jasmonic acid (JA),

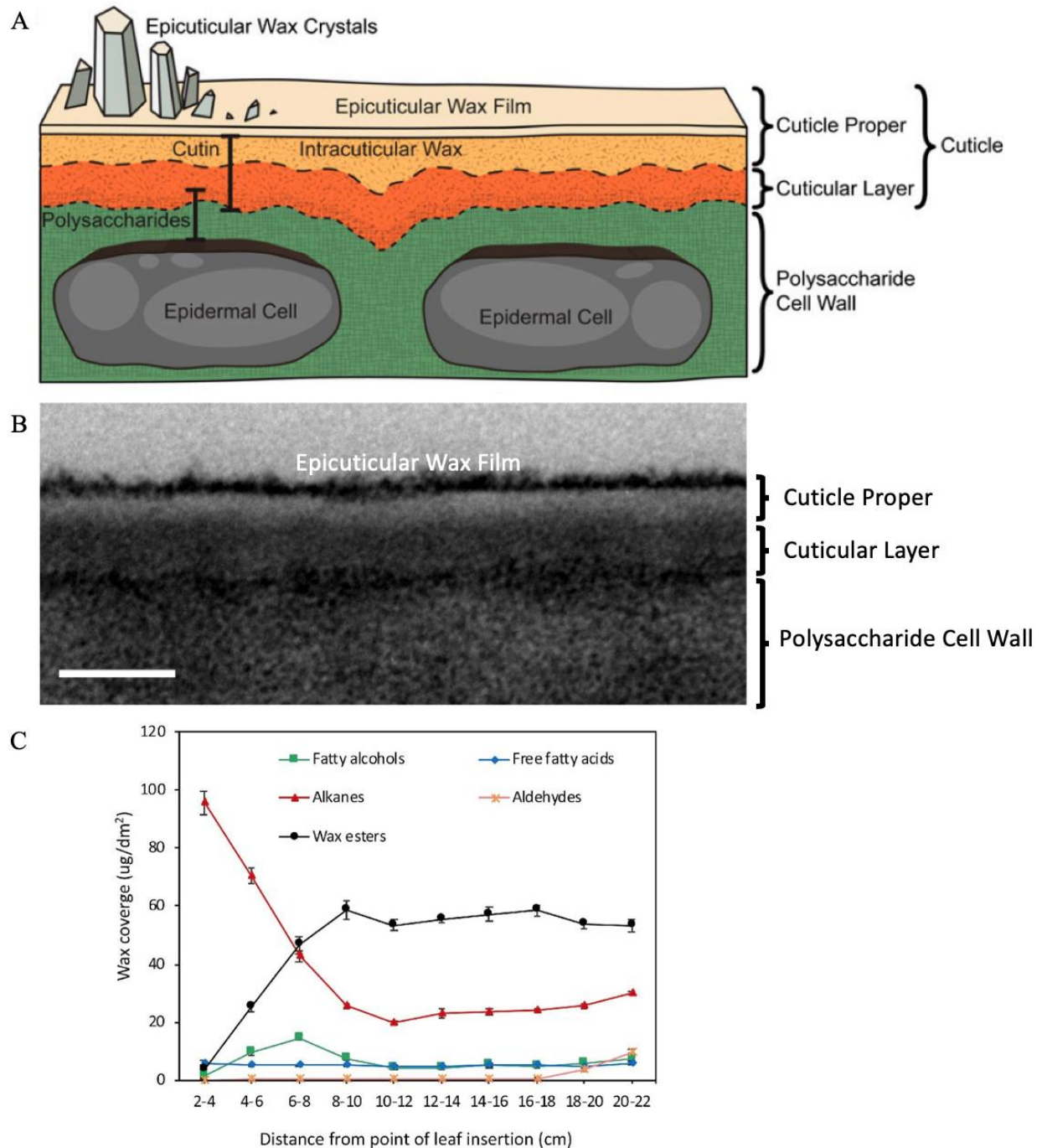
ethylene (ET)-response pathways, R gene upregulation (if the plant has corresponding R genes for the specific pathogen), mitogen-activated protein kinase (MAPK) signaling cascades and hypersensitive cell death (HR) at the localized infection site to minimize systemic pathogen spread (Glazebrook 2005). Some pathogens secrete effector molecules upon infection, which suppress immunity-related signaling pathways. Plants able to recognize effector molecules can mount an ETI response, which is an amplified PTI response that leads to HR (Glazebrook 2005).

### **Plant cuticle background: Structure, composition and development**

For many aerial plant pathogens, their initial interaction with the plant occurs at the cuticle, which provides the first physical defense against invading microbes. The plant cuticle is a waxy, hydrophobic coating found on all aerial non-woody plant tissue and serves as a physical barrier protecting the plant from environmental stresses including pathogen infection, dehydration, and UV radiation (Yeats and Rose 2013). Scientists have used scanning and transmission electron microscopy (SEM and TEM), gas chromatography and mass spectrophotometry (GC/MS) to study its general structure and chemical composition in *Arabidopsis thaliana* and other plant species. The cuticle contains two major components: 1) cutin, which serves as a structural framework for the cuticle, and 2) long-chain hydrophobic wax compounds embedded into the cutin polymer matrix (intracuticular wax), or on top of the cutin layer (epicuticular wax) (Fich *et al.* 2016; Yeats and Rose 2013). The cuticle organizes into three layers (Figures 1.1A, 1.1B). The cuticular layer is found immediately outside the cell walls of leaf epidermal cells, and contains a mix of polysaccharides, wax compounds and cutin. The cuticle proper is on top of the cuticular layer and consists of wax compounds and cutin. Lastly, the epicuticular layer is the outermost layer and forms a thin film over the cuticle and can sometimes contain epicuticular wax crystals. Primary literature reveals that cuticle structure and chemical composition can vary across different plant

species, organs, developmental stages of the plant or the leaf, or even different inbred lines or ecotypes of the same species grown in different environments, and these changes are not well understood (Jenks and Ashworth 2010).

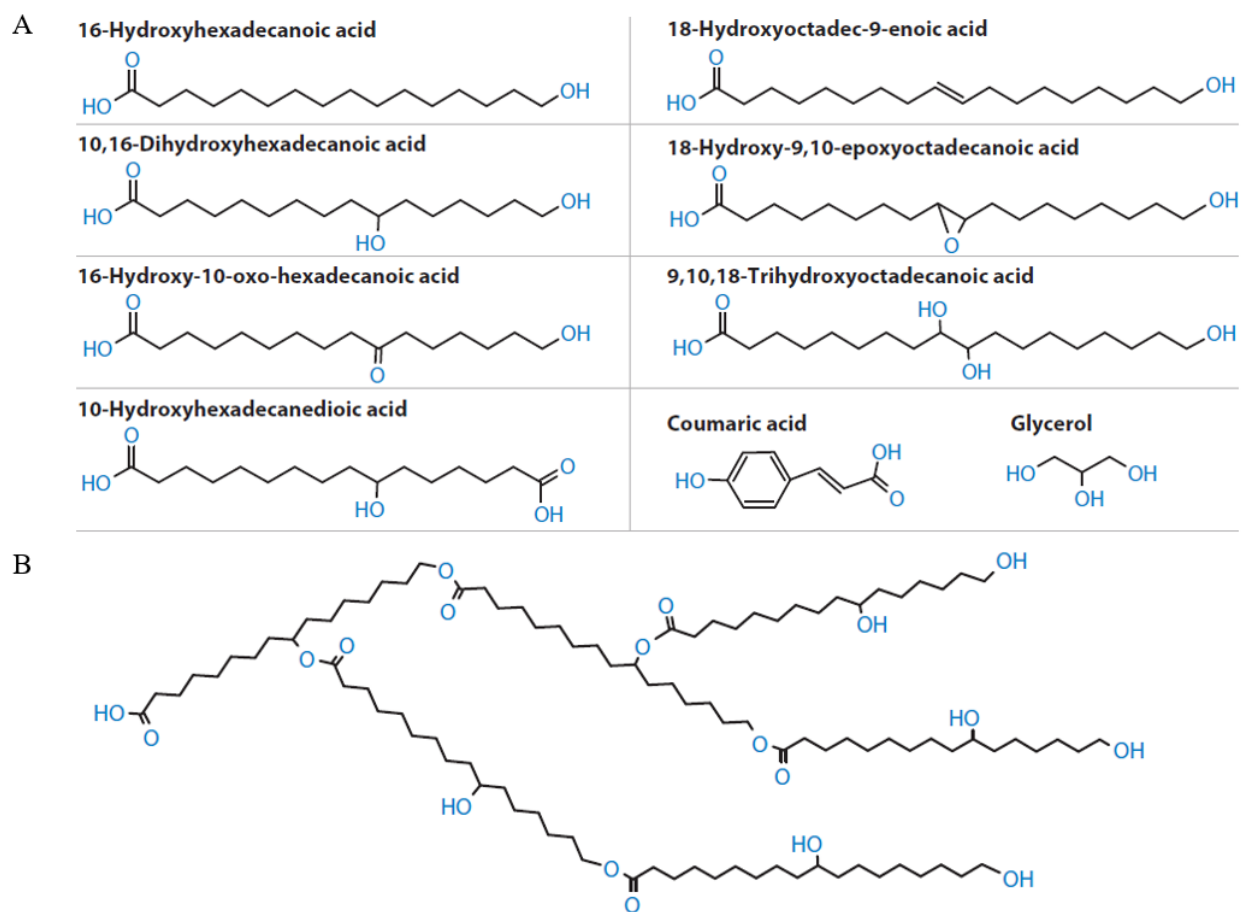
New, unpublished studies by our collaborators on the developmental gradient of maize cuticle have determined its chemical composition in inbred B73 during the transition period between juvenile and adult leaf tissue (Figure 1.1C). They found that wax esters and alkanes are the two most abundant cuticle wax components at the later adult stage (20-22cm), and their accumulation increases as the leaf develops away from the main stalk, whereas the concentration of fatty alcohols, free fatty acids and aldehydes remains relatively constant.



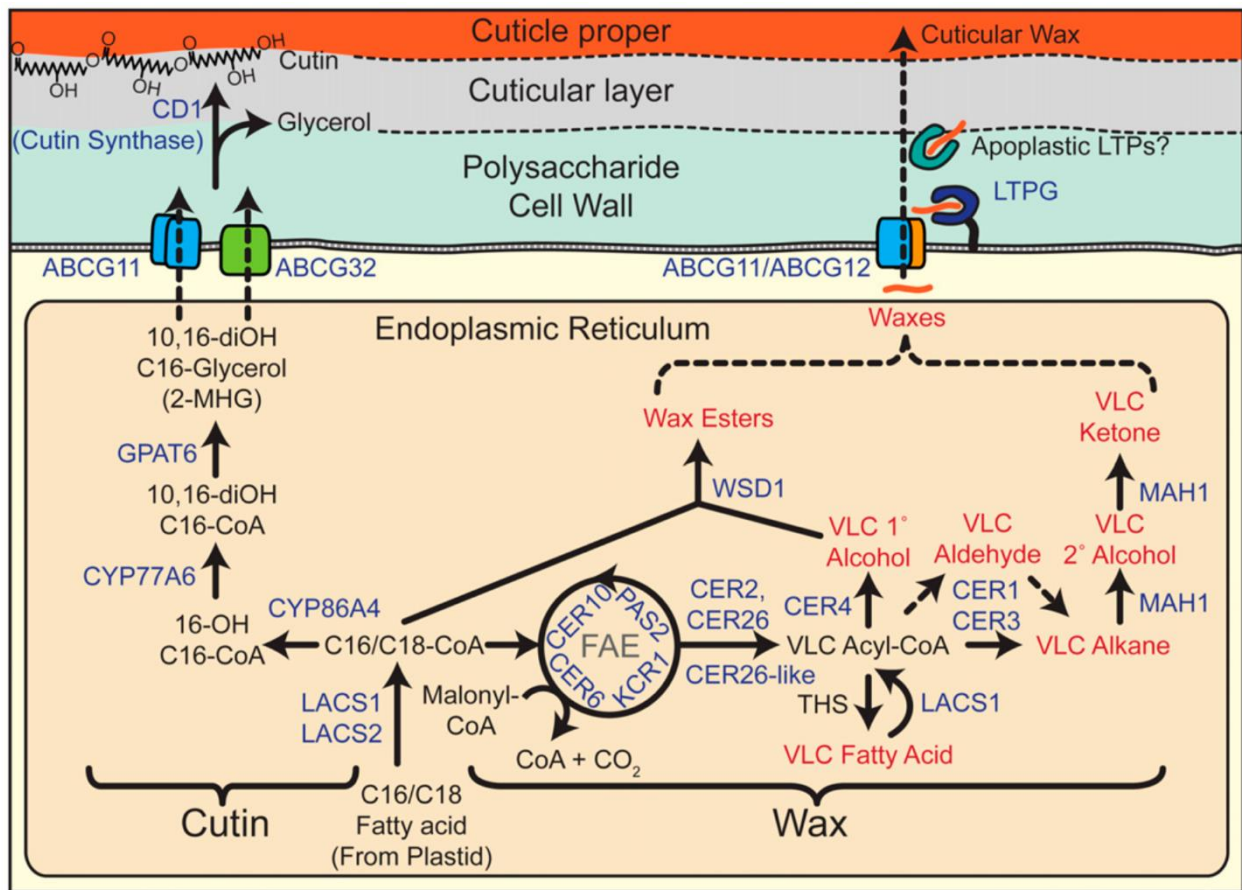
**Figure 1.1. Plant cuticle structure and wax composition.** (A) Plant cuticle structure diagram. Drawing not to scale (Modified from Yeats and Rose 2013). (B) Transmission Electron Microscopy image of mature B73 inbred maize leaf cuticle (Bourgault *et al.* 2019). Scale bar = 100nm. (C) Developmental gradient of cuticle wax profile of B73 inbred maize leaf. Adult leaf tissue wax profile is shown at 20-22cm distance from leaf insertion (Bourgault *et al.* 2019).



Cutin structure and composition visualization with TEM and analysis with X-ray diffraction, ester depolymerization and GC/MS reveal common cutin monomers found in the cuticle (Fich *et al.* 2016; Figure 1.2A). Further studies using molecular biology and nuclear magnetic resonance (NMR) on the *Arabidopsis thaliana* model reveal the genetic and biochemical control of cutin monomer biosynthesis, transport, deposition onto the leaf surface, and the polymerization and construction of cutin structure (Figure 1.2B, Figure 1.3). These events are largely mediated by long-chain acyl-CoA synthetases (LACSs), cutin synthases, ATP binding cassette-family transporters (ABCG-transporters), and extracellular polymerization enzymes known as glycine-aspartic acid-serine-leucine (GDSL) motif lipases.

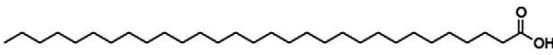
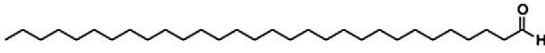
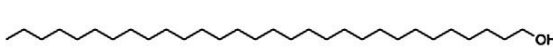
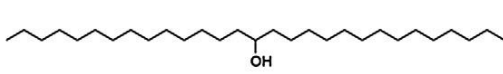

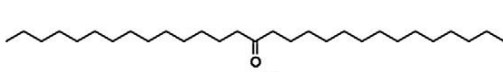
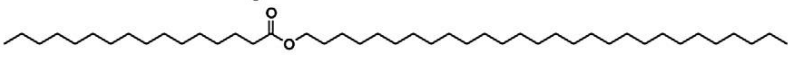


**Figure 1.2. Cutin chemical components and structure.** (A) Commonly found cutin monomers. (B) An example of cutin polymerization connected by ester linkages. (Modified from Fich *et al.* 2016).



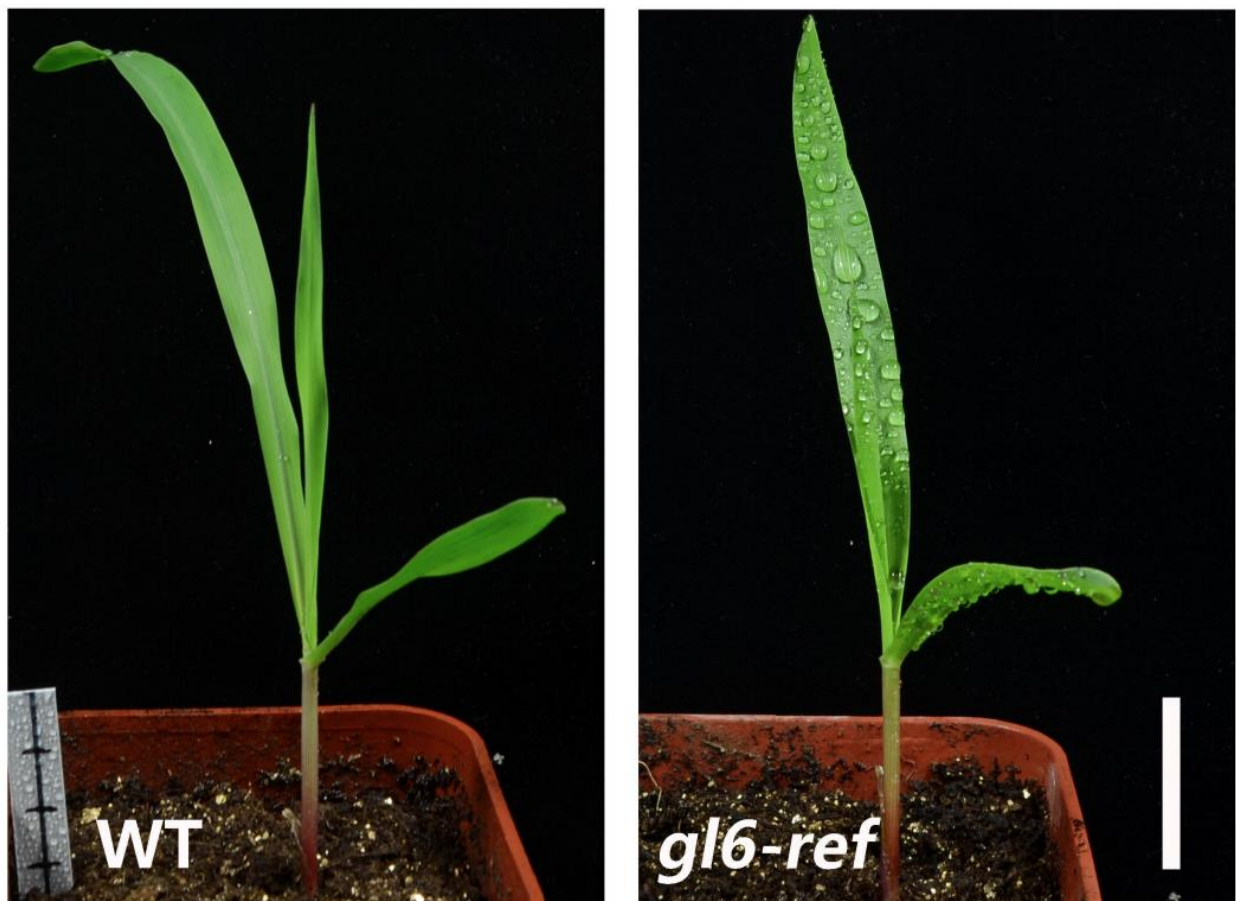
**Figure 1.3. Cutin and cuticle wax biosynthesis pathways.** Genes are noted in blue text, and wax classes are noted in red text. Gene symbol and gene name combinations are as follows: ABCG11 = ATP-BINDING CASSETTE G11, ABCG13 = ATP-BINDING CASSETTE G13, ABCG32 = ATP-BINDING CASSETTE G32, CD1 = CUTIN DEFICIENT 1, CER1 = ECERIFERUM1, CER2 = ECERIFERUM2, CER3 = ECERIFERUM3, CER4 = ECERIFERUM4, CER6 = ECERIFERUM6 CER10 = ECERIFERUM10, CER26 = ECERIFERUM26, CER26-like = ECERIFERUM26-like, CYP77A6 = CYP77A6, CYP86A4 = CYP86A4, GPAT6 = GLYCEROL-3-PHOSPHATE SN-2-ACYLTRANSFERASE6, LACS1 = LONG-CHAIN ACYL-COENZYME A SYNTHASE1, LACS2 = LONG-CHAIN ACYL-COENZYME A SYNTHASE2, LTPG = GPI-ANCHORED LIPID TRANSFER PROTEIN, MAH1 = MIDCHAIN ALKANE HYDROXYLASE1, WSD = WAX SYNTHASE/ACYL-COEZYME A:DIACYLGLYCEROL ACYLTRANSFERASE1 (Yeats and Rose 2013).

Cuticular waxes consist of fatty acids, aldehydes, primary/secondary alcohols, alkanes, ketones and wax esters, all varying in carbon chain lengths ranging from C20-C34 (Jetter *et al.* 2006, Figure 1.4). Unlike cutin, they are easily extractable with organic solvents, with chloroform being the most commonly used solvent in cuticle wax composition analyses (Fich *et al.* 2016). In addition, some plant species include antifungal and antibacterial compounds such as cyclic terpenoids, flavonoids and tocopherols in their cuticles (Zacchino *et al.* 2017). Cuticle wax biosynthesis occurs mainly in the endoplasmic reticulum of leaf epidermal cells and has been widely studied in the *Arabidopsis thaliana* model system. Synthesis begins with C16-C18 fatty acids, which then enter two separate metabolic pathways to synthesize: 1) primary alcohols and wax esters, 2) very-long-chain fatty acids (VLCFAs), aldehydes, alkanes, secondary alcohols, and ketones (Yeats and Rose 2013, Figure 1.3). While the intracellular trafficking of cuticle wax compounds to the membrane is unknown, ABCG-family transport proteins transport complete wax compounds into the cuticle space, where they are incorporated into the cutin matrix and form the intact cuticle (McFarlane *et al.* 2010).

Class of acyl lipid cuticular wax	Generic structure
Fatty acid	
Aldehyde	
Primary alcohol	
Secondary alcohol	
Alkane	
Ketone	
Wax ester	

**Figure 1.4. General wax classes commonly found in maize cuticle and their structures.** Average chain lengths shown. (Modified from Yeats *et al.* 2016).

Research on maize cuticle mutants beginning in the 1920s has since identified a panel of at least 26 different *glossy* mutants, defective in total wax load, wax composition or epicuticular wax deposition and are identifiable with a shiny, glossy appearance on juvenile maize leaves (Figure 1.5; Neuffer *et al.* 1997, Fan 2007). When sprayed with a thin mist of water, mutant leaves also show water adherence on their surface. Among the known 26 *glossy* maize mutants, only nine correspond to known genes (Table 1).

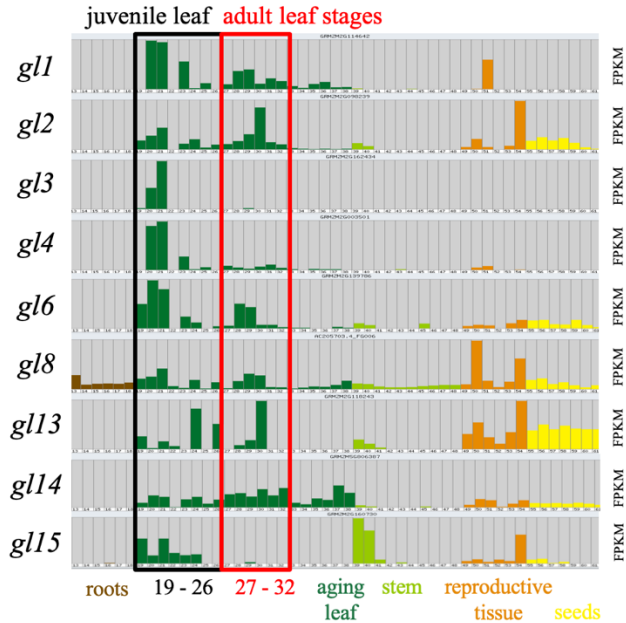


**Figure 1.5. Morphological example of a *glossy* mutant seedling's distinguishable phenotype.** Wild-type and *glossy* mutant seedlings were grown with leaf 3 sprouting from the whorl. A thin mist of water sprayed on wild-type vs. *gl6* seedlings result in water droplet adherence to *gl6* mutant's leaf surface. Scale bar: 3 cm (Li *et al.* 2019).

**Table 1.1. Published cloned *glossy* mutants and their proposed gene functions.**

<i>glossy</i> locus	Primary Literature Source	Proposed Gene Function
<i>gl1</i>	Stuaro <i>et al.</i> 2005	<i>Arabidopsis</i> WAX2 homolog, involved in cuticular wax biosynthesis and phospholipid transfer
<i>gl2</i>	Tacke <i>et al.</i> 1995	Acyl chain elongation from C30 to C32
<i>gl3</i>	Liu <i>et al.</i> 2012	Putative <i>myb</i> transcription factor involved in VLCFA biosynthesis gene expression
<i>gl4</i>	Liu <i>et al.</i> 2009	<i>Arabidopsis</i> CUT1 homolog, condensing enzyme in VLCFA biosynthesis
<i>gl6</i>	Li <i>et al.</i> 2019	Intracellular epicuticular wax trafficking
<i>gl8a/gl8b</i>	Xu <i>et al.</i> 2002 Dietrich <i>et al.</i> 2005	$\beta$ -ketoacyl reductase of acyl-CoA elongase (fatty acid elongase) complex
<i>gl13</i>	Li <i>et al.</i> 2013	ABCG wax transport protein
<i>gl14</i>	Zheng <i>et al.</i> 2019	Putative membrane-associated protein
<i>gl15</i>	Moose and Sisco 1996	<i>APETALA2</i> -like transcription factor mediating maize developmental transition between juvenile- and adult-stage
GRMZM2G10875 ( <i>ZmCER8</i> )  (not considered as a <i>glossy</i> gene)	Zheng <i>et al.</i> 2019	<i>Arabidopsis</i> CER8 homolog. VLCFA modifier.

Investigations on cuticle compositions and functional analyses on drought tolerance or pathogen resistance using *glossy* mutants is limited to juvenile-stage maize. During the transition from juvenile to adult-stage maize, the cuticle wax composition changes, with the notable decline in alkane content and the rise in wax ester content (Figure 1.1C). In addition, the deposition of epicuticular wax crystals is lost as the plant matures (Lawson and Poethig 1995). Because this area of research is largely unexplored for adult-stage plants and many known maize *glossy* genes are actively expressed during this agronomically important stage (Figure 1.6), we became interested in wax composition and functional analysis on adult *glossy* mutants. For our analysis, we chose *gl1*, *gl2*, *gl6*, *gl8*, and *gl14* from the known *glossy* genes because of their active expression in both juvenile- and adult-stage maize, and included *gl11*, *gl17*, and *gl18* as their gene products and expression are still unknown (Figure 1.6, Sekhon *et al.* 2011, Stelpflug *et al.* 2016).



**Figure 1.6. Tissue-specific RNA expression profile for known glossy genes in inbred B73.** 79 distinct tissue samples are included in the RNA-seq gene expression atlas (not all shown). Juvenile leaf tissues are outline with a black box, and adult leaf tissues are outlined in red. FPKM values for gene expression histograms and data from NimbleGen Microarrays and RNA sequencing are taken from MaizeGDB.org (Sekhon *et al.* 2011, Stelpflug *et al.* 2016). Leaf samples: 19 = Coleoptile 6 days after sowing, 20 = Pooled leaves V1, 21 = Topmost leaf V3, 22 = Shoot tip V5, 23 = Tip of stage 2 transition leaf V5, 24 = Base of stage 2 transition leaf V5, 25 = Tip of stage 2 transition leaf V7, 26 = Base of leaf stage 2 transition leaf V7, 27 = Immature leaves V9, 28 = 8<sup>th</sup> leaf V9 field, 29 = 11<sup>th</sup> leaf V9, 30 = 13<sup>th</sup> leaf V9, 31 = 13<sup>th</sup> leaf VT, 32 = 13<sup>th</sup> leaf R2.

## Plant cuticle interactions with plant immune response and pathogens

In this study, we focus on the role of the cuticle in conferring resistance to fungal pathogens. The cuticle provides the plant with an initial physical defense barrier against invading microbes. Primary literature exploring plant-pathogen interaction has led to large-scale biochemical analyses mainly in the *Arabidopsis thaliana* model system involving plant immunity, including widely studied topics in PTI, ETI and chemical signaling pathways that upregulate immune response (ROS, SA, JA, ET, R genes). However, further evidence has been found linking the cuticle and mediation of these plant immune responses against pathogens (Aragón *et al.* 2017).

Within the past decade, increasing evidence supports the role of the cuticle and other cuticular lipid compounds in plant immune response. A study on *FAEI* (a fatty acid elongase) and its overexpression in *Arabidopsis thaliana* mutants showed a link between VLCFA accumulation and cell death in trichomes, suggesting that VLCFAs are important localized signaling molecules that trigger HR response (Reina-Pinto *et al.* 2009, Javelle *et al.* 2010). In a separate study, an *Arabidopsis thaliana acp4* (acyl carrier protein 4) mutant was shown to have impaired cuticular wax and cutin accumulation and fails to mount SAR, an immunity pathway potentially mediated by DIR1, a lipid transfer protein (Xia *et al.* 2009, Maldonado *et al.* 2002). Additional *Arabidopsis thaliana* cuticle mutants were tested (*lacs2*, *lacs9*, *cer1*, *cer2*, *cer4*) and they were unable to mount a SAR response to both virulent and avirulent *Pseudomonas syringae* infections. Physically altered cuticle and reduced levels of FFAs, alkanes and primary alcohols correlated with increased susceptibility to infection, suggesting that a functional cuticle is necessary for plant immunity pathways (Xia *et al.* 2009). In addition to MAMP/PAMP signaling, cutin monomers and other cuticle components can trigger ETI, but the molecular mechanism for this process remains unknown (Schweizer *et al.* 1996, Aragón *et al.* 2017).

The “phyllosphere” is the aerial region of plants immediately surrounding leaf surfaces that harbors microbial pools of bacteria, viruses and fungi (Aragón *et al.* 2017). To withstand environmental changes in temperature, humidity and radiation, microbes will colonize and aggregate on leaf surfaces for survival—in some cases, pathogenic bacteria will invade the plant tissue for nutrients. Although these mechanisms vary among microbial species, all microbes must overcome four general categories and challenges during initial stages of colonization that involve overcoming the physical plant cuticle barrier: 1) Microbes must recognize hydrophobic leaf surfaces to initiate colonization processes. 2) Microbes with naturally charged cell surfaces must



adhere to hydrophobic cuticle on leaf surfaces long enough to form aggregate structures to facilitate growth. For pathogenic microbes, the cuticle provides an initial defense as a physical barrier that microbes must overcome for plant tissue invasion (Pfeilmeier *et al.* 2016). 3) In addition to these first two obstacles, fungal conidia must germinate for further growth. 4) Lastly, invasive microbial pathogens must overcome the cuticle's physical barrier properties, which may occur by entry via open stomata or through enzymatic degradation of cuticle and direct penetration into the leaf epidermis (Pfeilmeier *et al.* 2016, Horbach *et al.* 2010).

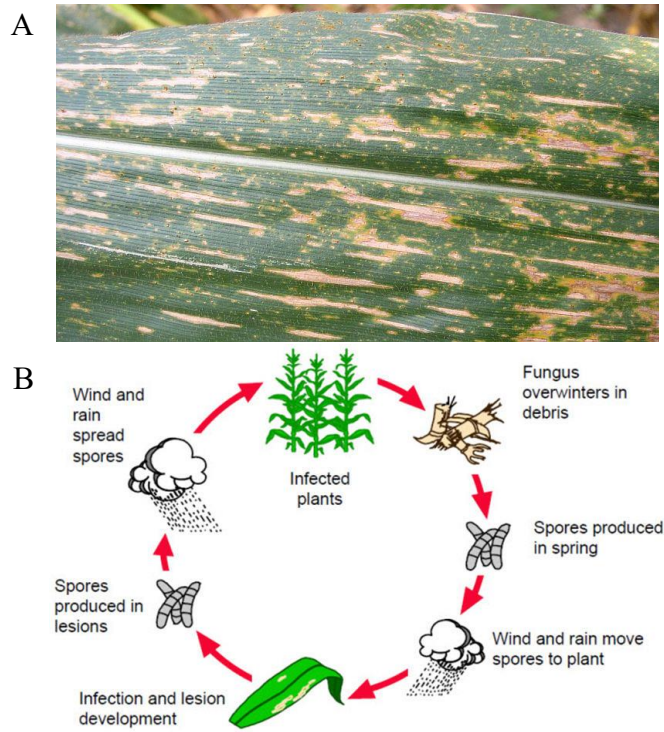
Some plant pathogens with charged cell surfaces secrete surfactants to aid in colonization on the hydrophobic cuticle. For example, *Pseudomonas syringae* is a well-studied pathogen against *Arabidopsis thaliana* and is a motile bacterium that secretes syringafactin, a natural surfactant that facilitates growth at the hydrophobic cuticular surface prior to invasion into the apoplast (Burch *et al.* 2011). In addition, many fungal pathogens like *Cochliobolus heterostrophus*, *Magnaporthe grisea*, *Blumeria graminis* and others secrete extracellular matrix adhesive materials or hydrophobic proteins to enable conidia to germinate without being removed from the leaf surface or other hydrophobic surfaces tested (Carver *et al.* 1999, Braun and Howard 1994). Aside from these examples, it is not widely known how pathogens accomplish the necessary interactions with mature cuticle for early-stage pathogenesis.

Cuticle composition and individual cutin or cuticular wax components are known to affect fungal pre-penetration processes like germination and appressoria formation, or initial invasion into leaf tissue (Hansjakob *et al.* 2011, Weihmann *et al.* 2016). Fungal appressoria are circular-shaped swellings arising from germ tubes that aid in adhesion and penetration of plant cells (Deising *et al.* 2000). Studies on *Arabidopsis thaliana* mutants (*cer1*, *cer3/wax2*, *lacs2*) with the pathogen *Colovinomyces orontii* showed that changes in cuticle composition were responsible for

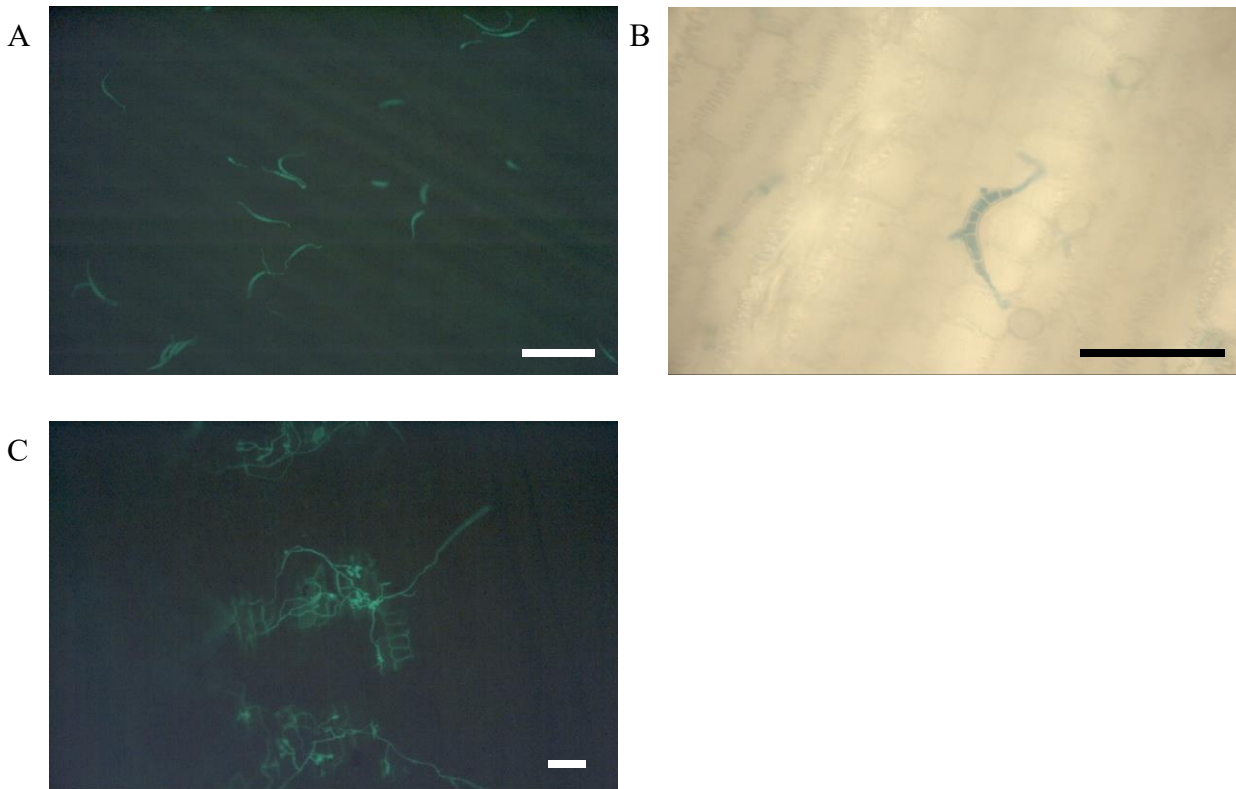
pre-penetration event modulation (Inada and Savory 2011). Further research with *Blumeria graminis* germination on barley *cer* mutants and maize *gll1* mutants demonstrated the role of individual cuticle wax components (hexacosanol, hexacosanal, VLCFAs) in promoting conidial germination within specific host-pathogen relationships (Zabka *et al.* 2008, Hansjakob *et al.* 2011). Additionally, conidial recognition of cutin C<sub>16</sub> monomers can induce production of cutinase enzyme, which digests cutin and further aids in attachment to the leaf surface and infection progression (Aragón *et al.* 2017). Other pathogens use enzymes to degrade the cuticle for entry, and wax-sensing receptors can promote gene expression to promote conidia germination and cuticle degradation (Doehlemann *et al.* 2006, Mendgen *et al.* 1996). Lastly, there are some studies relating cuticle thickness and permeability with changes in infection susceptibility. The *Arabidopsis thaliana* *acp4* and *glabrous1* (*gll*, not to be confused with maize *glossy1*) mutants showed decreased levels of cutin and wax components which led to increased susceptibility to *Botrytis cinerea* and *Pseudomonas syringae* infection (Xia *et al.* 2009). It is noted that the cuticle permeability and infection susceptibility relationship is largely variable, depending on which plant and pathogen model systems are being studied. For example, other *Arabidopsis thaliana* and tomato mutants like cytochrome P450-dependent oxidases (*CYP86A2*), *LACS2*, overexpressed *peroxidase 57* (*PER57*), alpha-beta hydrolase (BODYGUARD), and DEWAX transcription factor all showed increased leaf cuticle permeability (Ziv *et. al* 2018). All of these described mutants showed improved resistance against *B. cinerea*, but increased susceptibility to *P. syringae*.

## ***Cochliobolus heterostrophus*: Causal agent of Southern Corn Leaf Blight**

*Cochliobolus heterostrophus* is a necrotrophic fungus and is the main causal agent of Southern Corn Leaf Blight (SCLB) in *Zea mays* (Horwitz *et al.* 2013). Under normal conditions, SCLB is not a severe, destructive disease in the crop industry, but it became a widely studied pathogen after the 1970-1971 SCLB epidemic in the Midwestern United States. *C. heterostrophus* infection is identified by brown-colored, irregularly shaped lesions found on leaves, and is propagated by conidia and is spread agriculturally by wind and rain (“Southern Leaf Blight” 2010, Figure 1.7A). Upon landing on leaves under moist conditions, conidia germinate from both ends, produce appressoria that recognize the leaf surface, and begin a rapid adhesion process that involves secretion of a fastidious adhesion matrix (Horwitz *et al.* 2013, Braun and Howard 1994, Figure 1.8). Surprisingly, while *C. heterostrophus* produces appressoria, these common adhesion organs are unnecessary for *C. heterostrophus* adhesion to or penetration through the leaf surface (Horwitz *et al.* 1999). Hyphae directly penetrate through the cuticle and into the epidermis, causing cell death symptoms. Notably, entry can also occur through open stomatal pores. Unfortunately, little is known about *C. heterostrophus* interaction with the plant cuticle, aside from one study connecting low cuticle thickness and low epicuticular epoxides with enhanced *C. heterostrophus* infection (Lequeu *et al.* 2003).



**Figure 1.7. Agricultural symptoms and life cycle of *C. heterostrophus*.** (A) Necrotic lesions caused by *C. heterostrophus* found on maize leaf surfaces (Modified from “Southern Leaf Blight” 2010). (B) Life cycle of *C. heterostrophus*. (Modified from “Southern Leaf Blight” 2010).

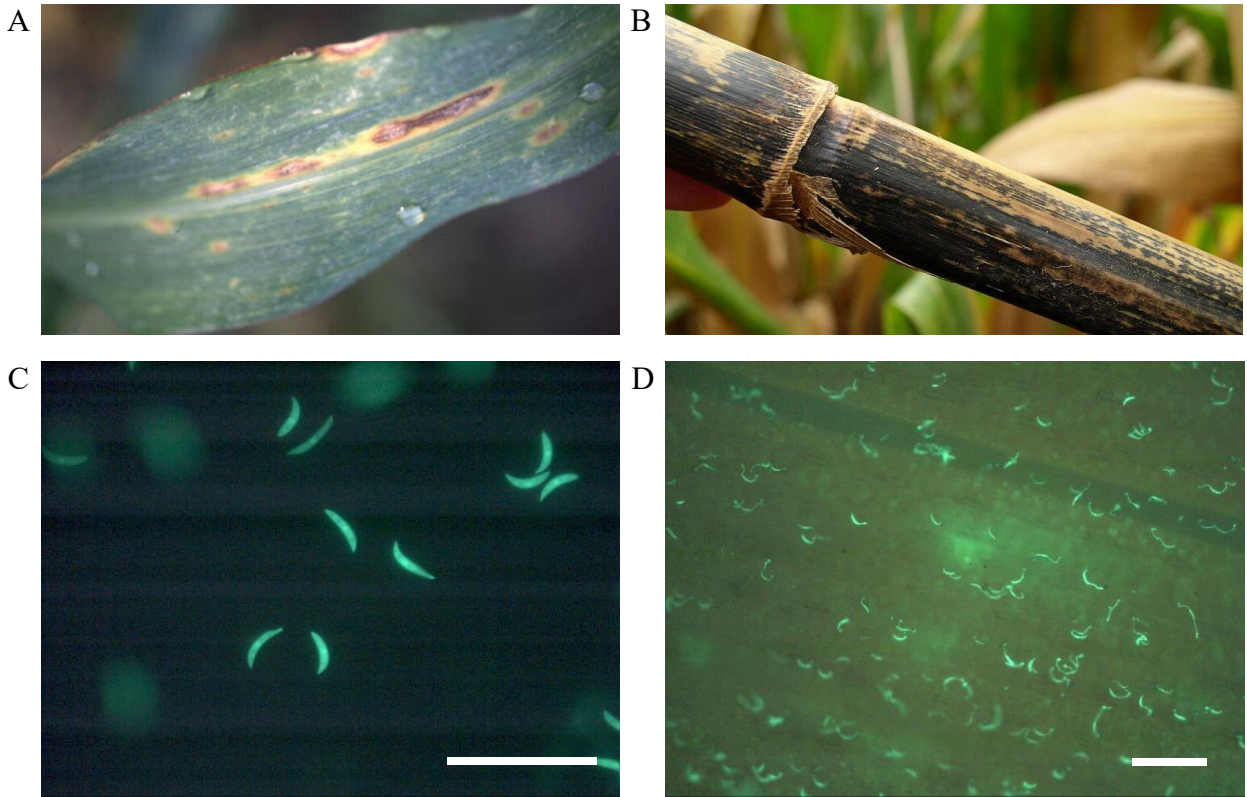


**Figure 1.8. *C. heterostrophus* infection on maize leaf surfaces.** (A) GFP-labelled conidia deposited on leaf surface shown 1-hour post-infection (hpi) at 200x magnification. (B) Germinated conidia fixed at 1-hour post-infection (hpi) and stained in 0.1% aniline blue shown at 400x magnification. (C) GFP-labelled growth on leaf surface 24 hpi shown at 100x magnification (Unpublished lab data). Scale bars shown: 100  $\mu\text{m}$ .

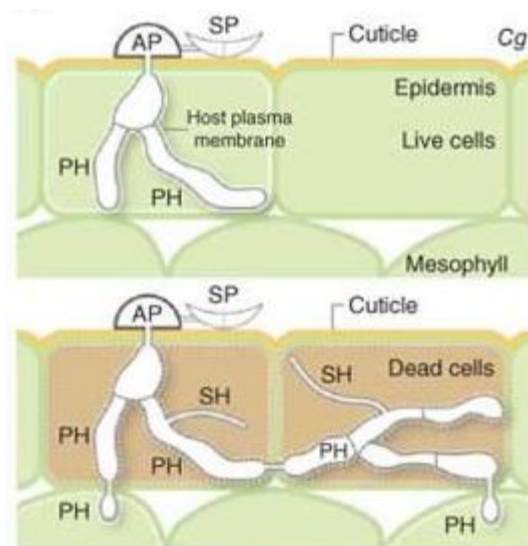
## ***Colletotrichum graminicola*: Causal agent of Anthracnose Stalk Rot**

*Colletotrichum graminicola* is a hemibiotrophic fungus and is the main causal agent of Anthracnose Stalk Rot in *Zea mays* and can be characterized with mild lesion formation on leaves during early-stage infection and severe rotting of the stalk during late-stage infection (Mims *et al.* 2002, Bergstrom and Nicholson 1999, “Anthracnose Stalk Rot” 2013, Figure 1.9A, Figure 1.9B). Notable epidemics were recorded in Illinois and the Midwestern United States in 1972, 1982 and 1983, and can still be found regularly worldwide (Warren *et al.* 1973, Vernard 2006, Anderson 1987).

When *C. graminicola* conidia land on the leaf surface under humid conditions, they germinate and form appressoria (Figure 1.9C, Figure 1.9D). Conidia recognition of hydrophobic surfaces induces appressoria formation, leads to tight adhesion to the leaf cuticle and is necessary for disease progression (Braun and Howard 1994, Mercure *et al.* 1994, Apoga *et al.* 2004). During initial stages of *C. graminicola* infection, hyphae emerging from appressoria penetrate through the plant cuticle by mechanical force directly downwards with the help of digestive enzymes (cutinase, cellulase, pectinase, polygalacturonase) that break down cuticle components (Venard 2006, Pascholati *et al.* 1993). During the biotrophic phase, primary host cells emerge from the invading hyphae and begin colonizing epidermal cells, which are initially kept alive while the organism propagates. Following the biotrophic phase, the infection enters the necrotrophic phase, where secondary hyphae emerge from the primary hyphae and the plant begins showing visible infection symptoms and cell death (Politis *et al.* 1973, Figure 1.10).



**Figure 1.9. Maize infected with *C. graminicola*.** (A) Early stages of infection on maize leaves (B) Late stage infection with black coloration and rotting on maize stalk (“Anthracnose Stalk Rot”). (C) GFP-*C. graminicola* conidia shown at 400x magnification. (D) GFP-*C. graminicola* on a maize leaf surface 2 days post-infection shown at 200x magnification (Unpublished lab data). Scale bars shown: 100  $\mu$ m.



**Figure 1.10. *C. graminicola* infection process.** SP: spore. AP: appressorium. PH: biotrophic primary hyphae. SH: necrotrophic secondary hyphae. Biotrophic phase of infection is limited to primary hyphae development shown in the top image, whereas necrotrophic phase includes secondary hyphae shown in the bottom image (Modified from O’Connell *et al.* 2012).

## **Our project**

The focus of this project is to characterize the relationship between adult maize leaf cuticle and the fungal pathogens *C. heterostrophus* and *C. graminicola*. Among the vast quantity of maize pathogens, these two were selected as vehicles to study cuticle-pathogen interaction because they penetrate through the cuticle and we obtained GFP-labelled strains of these pathogens for ease of visualization under an epifluorescent microscope. Prior studies performed on maize and these two fungi provide insight for assay development to quantify and attribute changes in infection susceptibility of wild-type and *glossy* mutant maize to differences in cuticle composition and/or cuticle-mediated infection progression. However, the limitations of current research include the following two points: 1) Maize used in these studies use juvenile-stage plants, which are agronomically less significant and show substantial differences in cuticle structure compared to their adult-stage counterparts, and 2) *glossy* mutants studied were obtained from the Maize Genetics Cooperation Stock center and did not have a common wild-type background for comparison. We completed multiple generations of introgression on a panel of diverse *glossy* mutants (*gl1*, *gl2*, *gl6*, *gl8*, *gl11*, *gl14*, *gl17*, *gl18*) into W22-inbred background to perform our studies on adult-stage maize plants (Figure 1.6, Table 1).



**Plant material****Table 2.1. *glossy* genotype panel allele and stock identities with introgression status into W22 background.**

<i>glossy</i> mutant/allele	Maize Genetics Cooperation Stock Number	Backcrosses into W22
W22 (wild-type)	-	-
<i>gl1</i>	709A	4
<i>gl2</i> -Salamini	208H	4
<i>gl6</i>	313A	4
<i>gl8</i> -R	518BA	4
<i>gl11</i>	215B	3
<i>gl14</i>	215A	4
<i>gl17</i>	501E	3
<i>gl18</i> -g	801A	4

Lines of maize used include: Wild-type W22, *gl1*, *gl2*, *gl6*, *gl8*, *gl11*, *gl14*, *gl17*, and *gl18*. *glossy* mutants were introgressed into W22 background via three (*gl11*, *gl17*) or four (*gl1*, *gl2*, *gl6*, *gl8*, *gl14*, *gl18*) backcrosses (Table 2). Greenhouse replicate studies were performed with plants grown under 16h/8h light/dark greenhouse conditions during non-summer seasons. Field-grown replicate studies were performed with plants organized in 12-plant plots randomly placed in a field in San Diego, California at UC San Diego's biology field station, surrounded by border lines during the summer season. Plants were grown to adult-stage with a minimum of leaf 9 fully expanded with the leaf sheath visible as qualification for fungal infection assays.

**Fungal strains and growth conditions**

Strains of GFP-labelled *Cochliobolus heterostrophus* (provided by Dr. Gillian Turgeon, Cornell University, USA through Dr. Peter Balint-Kurti, North Carolina State University, USA) and GFP-labelled *Colletotrichum graminicola* (provided by Dr. Serenella Sukno, University of Salamanca, Spain) were cultured on Potato Dextrose Agar (PDA). Stocks of fungal conidia were stored with autoclaved skim milk on sterile-heated silica gel beads under -80°C conditions. Beads

were plated on V8 juice agar (0.54% w/v CaCO<sub>3</sub>, 2% w/v Agar, 20% v/v Campbell V8 Vegetable Juice, 80% v/v ddH<sub>2</sub>O) for a minimum of 48 hours under 24-hour light conditions. A 0.25 cm<sup>2</sup> area of the V8 juice agar plate was transferred onto PDA (Difco), sealed with two layers of Parafilm® (Bemis #PM-996), and was grown for 14 days under 24-hour light conditions at 25°C. Special care was taken to ensure the fungal incubation time on plates was minimized to ensure pathogenicity of both pathogens.

### **Long-term fungal infection assays on detached adult maize leaves**

Full length adult-stage leaves (generally leaf 9 or higher) were harvested by cutting at the leaf base. Two layers of Kimtech Kimwipes (Kimberly-Clark #34155) were fully saturated with ddH<sub>2</sub>O and placed inside 100 x 15mm square petri dishes (Genesee Scientific #26-275). Leaves were divided into three portions along the leaf, and a section of the middle third section was excised to fit the area of the petri dish. Three biological replicates for each genotype were used.

Prior to infection, sterile-filtered 0.05% Tween 20 was prepared and stored at 4°C. Two PDA plates of the appropriate fungal strain were harvested by applying ice-cold 5 mL sterile-filtered 0.05% Tween 20 per plate. Spores were loosened in liquid using sterilized cotton swabs and the suspension was filtered through four layers of autoclaved cheesecloth. The fungal inoculum concentration was adjusted to 1x10<sup>6</sup> conidia/ml using a hemocytometer. 5 µl droplets of the infection inoculum were applied along the surface of the leaf. Petri dishes were sealed with two layers of Parafilm® and were exposed to 24-hour light conditions. Symptom analysis with visual inspection and protein extraction with GFP fluorescence quantification was performed at 0, 2, and 6 days post-infection (dpi) for *C. heterostrophus*, and 0, 2, and 8 dpi for *C. graminicola*.

Leaf infection images were taken with leaves inside their square petri dishes. The lid was wiped clear of all condensation. Photos were shot with a OnePlus 5, about 2 feet above the sealed

petri dish, and with a 20cm x 40cm cardboard covering placed behind the camera. Overhead backlighting was provided with long fluorescent tube lights.

### **Fungal adhesion rate quantification**

Leaf pieces were prepared in square petri dishes as described above. Fungal suspensions were prepared as described above, taking special care to ensure fungal suspensions were held on ice prior to placement of inoculum droplets on leaf surfaces. The fungal inoculum concentration was adjusted to  $2 \times 10^4$  conidia/ml using a hemocytometer. 5  $\mu$ l droplets of the inoculum were applied onto the leaf surface as described above and were marked with a permanent lab marker. Plates were covered with the petri dish cover and were left under total light conditions for 2 (*C. heterostrophus*) or 4 (*C. graminicola*) hours.

Three 250 ml beakers were filled with 175 ml of 0.05% Tween 20 and placed in sequence. Leaves were submerged five times in each beaker. After submersion, droplet sites were excised and visualized under GFP excitation and emission settings on an epifluorescent microscope at 200x magnification covering the whole droplet in one view field (Nikon Eclipse TE2000-U, QImaging Inc. Retiga 2000R Camera, QImaging Inc./Media Cybernetics Inc. QCapture Pro Version 6.0). Quantitative analysis was performed by taking an image of the droplet infection site, manual counting of all conidia inside each view field's fluorescent image with ImageJ software and with 24 droplet sites per genotype on three biological replicates.

### **Leaf piece homogenization with protein extraction and GFP fluorescence quantification**

At the appropriate time point in a long-term fungal infection assay, leaf droplet infection sites were excised using a fixed-size (1 cm radius) cork borer. Leaf pieces were placed inside a 2 ml microcentrifuge tube with two tungsten metal beads and homogenized with liquid nitrogen and a mixer mill machine (1 minute, 25 Hz, Retsch #20.745.0001). 0.6 ml of freshly prepared protein

extraction buffer (30 mM Tris-HCl pH 8, 10 mM EDTA, 10 mM NaCl, 5 mM DTT) was added to each sample and was thoroughly suspended and thawed over ice. Samples were centrifuged (15 minutes, 15,000g, 4°C), and 200 µl of supernatant of each sample was placed into a clear 96-well plate. Samples were visualized with GFP excitation and emission settings on a 96-well microplate reader (Synergy H1 Hybrid #1411111 with Blue/Green Filter Cube, BioTek Instruments Gen5 Software Version 2.06.10). Quantitative analysis was performed using 6 droplet infection sites per genotype on three biological replicates at each designated time point.

### **Leaf cuticle wax analysis**

Cuticle wax extraction and GC/MS analysis was performed by a collaborating lab (Dr. Isabel Molina and Dr. Richard Bourgault, Algoma University, Canada). Methods used were provided and performed by Dr. Bourgault.

Leaf material (Wild-type inbred W22, *glossy* panel) was harvested in San Diego, California. 14-15 cm pieces from the middle portion of adult leaves were packed in three layers of paper towels, fully hydrated with ddH<sub>2</sub>O and shipped to Algoma University, Canada, where they were frozen until wax extraction.

All glassware was pre-rinsed with chloroform. Two sizes of Pyrex glass tubes and PTFE-lined caps were used: Pyrex 9826-20 (25 mL) tubes for extraction and Pyrex 9826-13 (9 mL) caps for collection and derivatization. After thawing, an 8 cm length of leaf from one side of the midrib was removed using a scalpel and the rest of the leaf pieces were discarded. Leaves were gently blotted dry and inserted into a 25 mL collection tube with 8 mL chloroform. The tube was shaken gently for one minute, and the chloroform-wax suspension was transferred into a 9 mL collection tube containing 5 µg internal standards (C15:0 primary alcohol, C17:0 free fatty acid, C24:0 alkane). The 9 mL collection tube was briefly mixed and the solvent dried using N<sub>2</sub> gas. The

residue was derivatized using 100  $\mu\text{L}$  each of pyridine and N,O-Bis(trimethylsilyl) trifluoroacetamide (Sigma), and heated for 10 minutes at  $100^\circ\text{C}$ . The reactants were dried using  $\text{N}_2$  gas, and the residue was suspended in hexane for GC analysis.

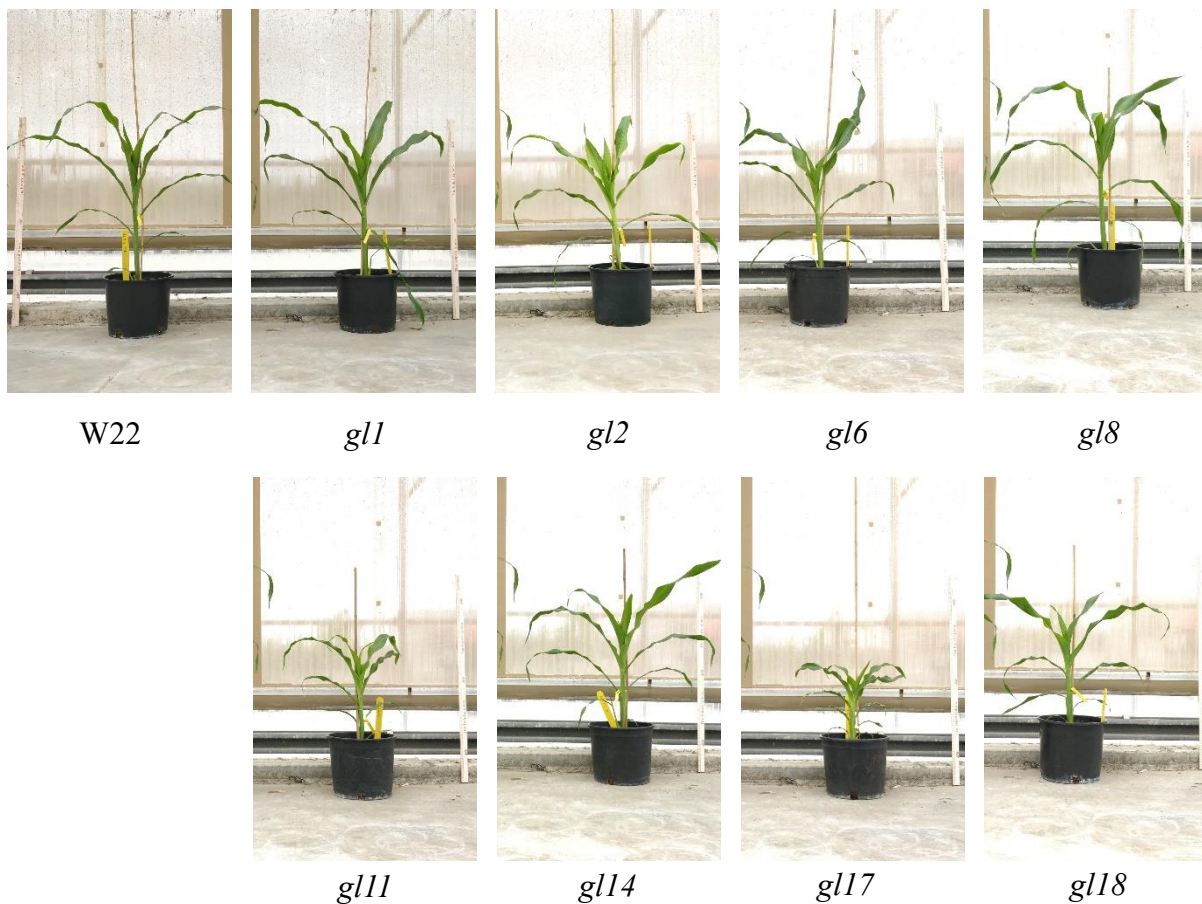
## CHAPTER 3: Results

### **A. *gl11* and *gl17* mutants are more susceptible to *C. heterostrophus* infection**

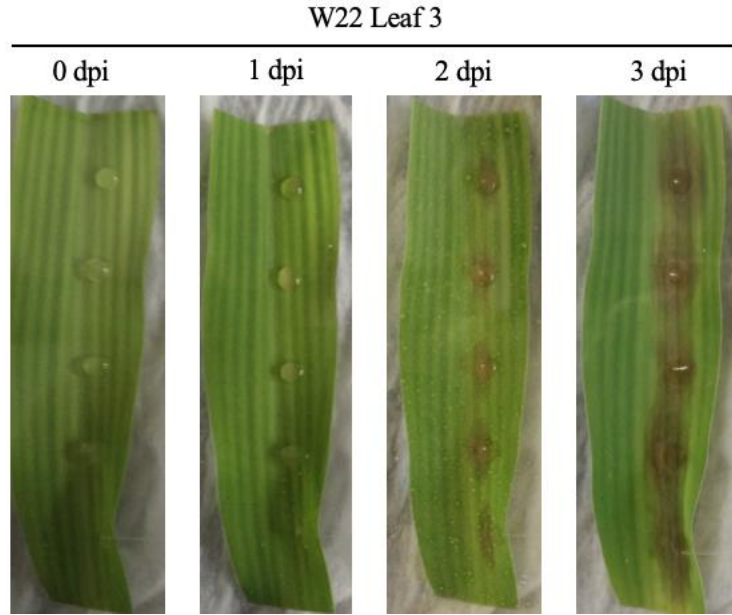
To study the role of adult maize cuticle in providing resistance to fungal pathogens, we performed pathogen assays on a chosen panel of maize *glossy* mutants with known *glossy* gene expression in adult-stage maize (*gl1*, *gl2*, *gl6*, *gl8*, *gl14*) or *glossy* mutants with unknown genes (*gl11*, *gl17*, *gl18*), which all show cuticular wax deposition defects in juvenile stage (Figure 1.6, Table 2). At the time of this study, *gl6* and *gl14* were unknown but were later cloned by others (Li *et al.* 2019, Zheng *et al.* 2019). During optimization of the detached leaf infection assay for adult maize leaves (leaf 9+), we observed that two mutants, *gl11* and *gl17*, displayed a stunted growth phenotype compared to wild-type W22 during adult stage, but still developed comparable adult leaves (Figure 3.1). It was noted that *gl11*'s stunted growth phenotype may have been exacerbated by a tendency for developing leaves to remain unrolled in the whorl (described in Neuffer *et al.* 1997 as a “leaf adherence” phenotype), and greater care to aid the plant in unrolling juvenile leaves during its growth was necessary (picture not shown). We hypothesized that these adult mutants with deficient cuticular waxes would show changes in infection susceptibility to *C. heterostrophus*. Previously described *C. heterostrophus* infection assays showed visible lesion formation on juvenile (leaf 3) leaves over a 6-day infection time course (Degani 2014). To confirm these results, we examined *C. heterostrophus* infection on juvenile wild-type W22 leaves and observed early signs of necrotic lesion formation in the middle of the droplet infection sites 1 dpi (Figure 3.2).

Then, we performed a series of infection assays on our genotype panel grown to adult-stage (W22, *gl1*, *gl2*, *gl6*, *gl8*, *gl11*, *gl14*, *gl17*, *gl18*; Figure 3.3). We observed early lesion development 2 dpi on all genotypes and varying levels of lesion progression by 6 dpi. *gl11* and *gl17* mutants seemed to have darker lesions than other genotypes. To quantify the amount of fungal growth at

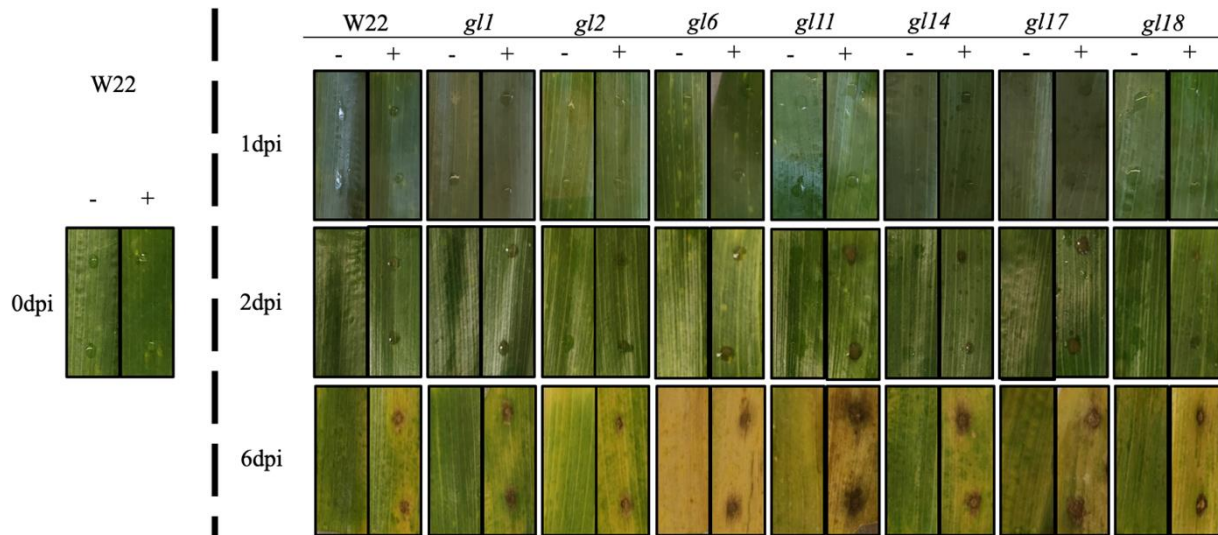
droplet infection sites, we performed a protein extraction and GFP fluorescence quantification of homogenized, fixed-size infection sites on our assorted genotypes at 1 and 6 dpi (Figure 3.4). No significant changes were observed between 0 and 1 dpi within and across genotypes (data not shown). However, we found significant differences in GFP fluorescence quantity across the genotype panel between 1 and 6 dpi, and *gl11* and *gl17* mutants showed consistently higher GFP quantity by roughly 25% at 6 dpi compared to wild-type. Therefore, we concluded that *gl11* and *gl17* mutants were more susceptible to *C. heterostrophus* infection. Although *gl1*, *gl2*, and *gl6* showed lower GFP load in our first experiment, we did not have sufficient evidence across multiple replicates to confidently conclude anything about their infection susceptibility (Figure 3.4A).



**Figure 3.1. Adult-stage W22 and glossy mutants grown under greenhouse conditions. Scale bar = 1 meter.**

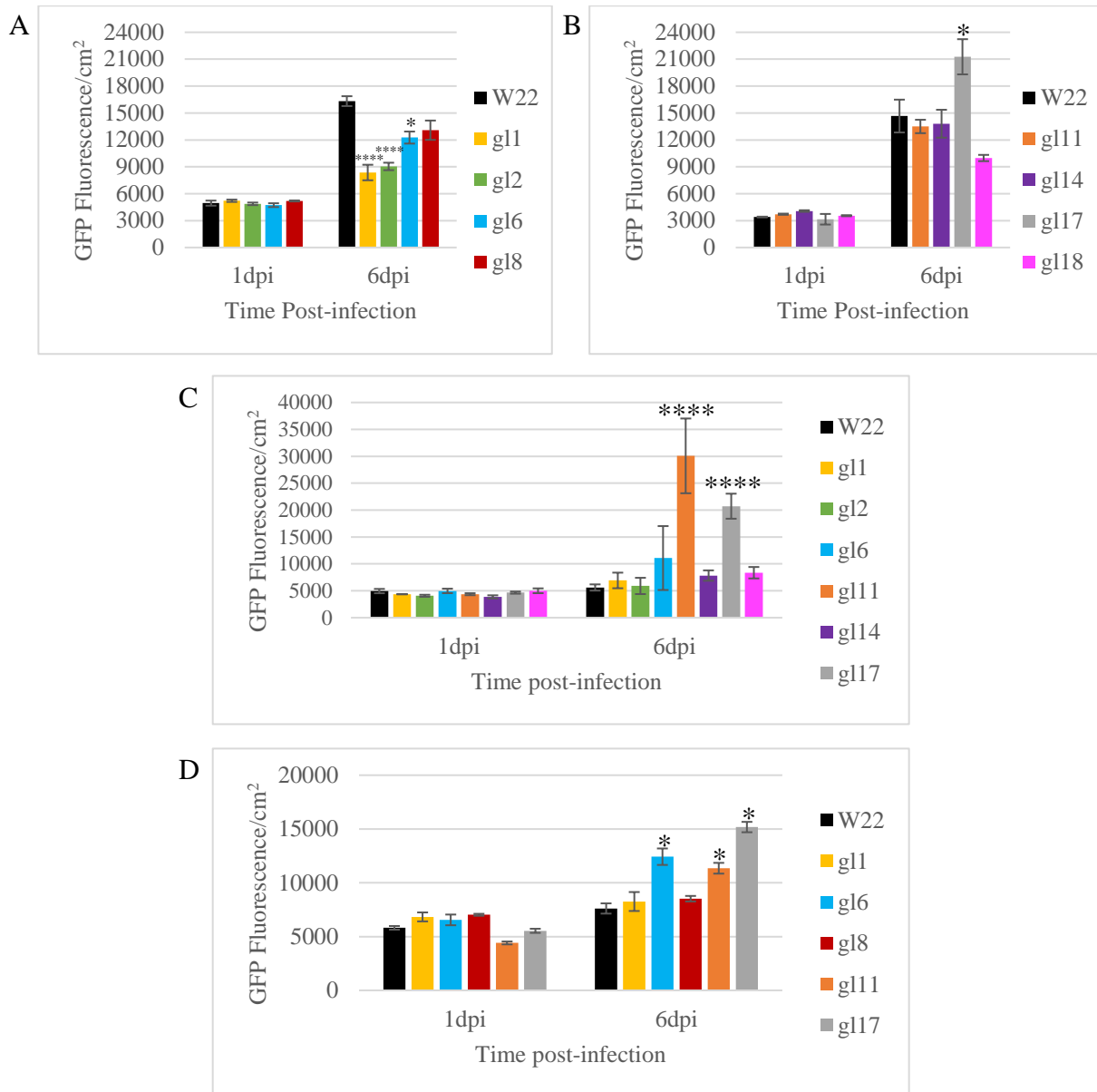


**Figure 3.2 Juvenile wild-type W22 leaves infected with *C. heterostrophus*.** A  $1 \times 10^6$  *C. heterostrophus* conidia/ml in 0.05% Tween 20 infection monitored over a 3-day time course. Gradual lesion formation with faint, light brown coloration starting from the middle of each droplet infection site is observed. Experiment was repeated three times, with representative results shown.



**Figure 3.3. Visual disease progression of W22 and *glossy* mutant detached leaves infected with *C. heterostrophus*.** 5  $\mu$ l droplet infection sites on detached adult leaf surfaces from the *glossy* panel were monitored over a 6-day time course. (-): Mock infection with 5  $\mu$ l droplets of sterile 0.05% Tween 20. (+): Infection with 5  $\mu$ l droplets of  $1 \times 10^6$  *C. heterostrophus* conidia/ml in 0.05% Tween 20. Panel shows results from one infection performed on the largest *glossy* panel, and three other experiments follow the same trend. Initial lesion formation is observed 2 dpi, with varying levels of lesion formation at 6 dpi. 0 dpi infection photos for *glossy* mutants are not shown, as all leaves show the same visual behavior as wild-type W22. Experiment was repeated four times, with representative results shown.





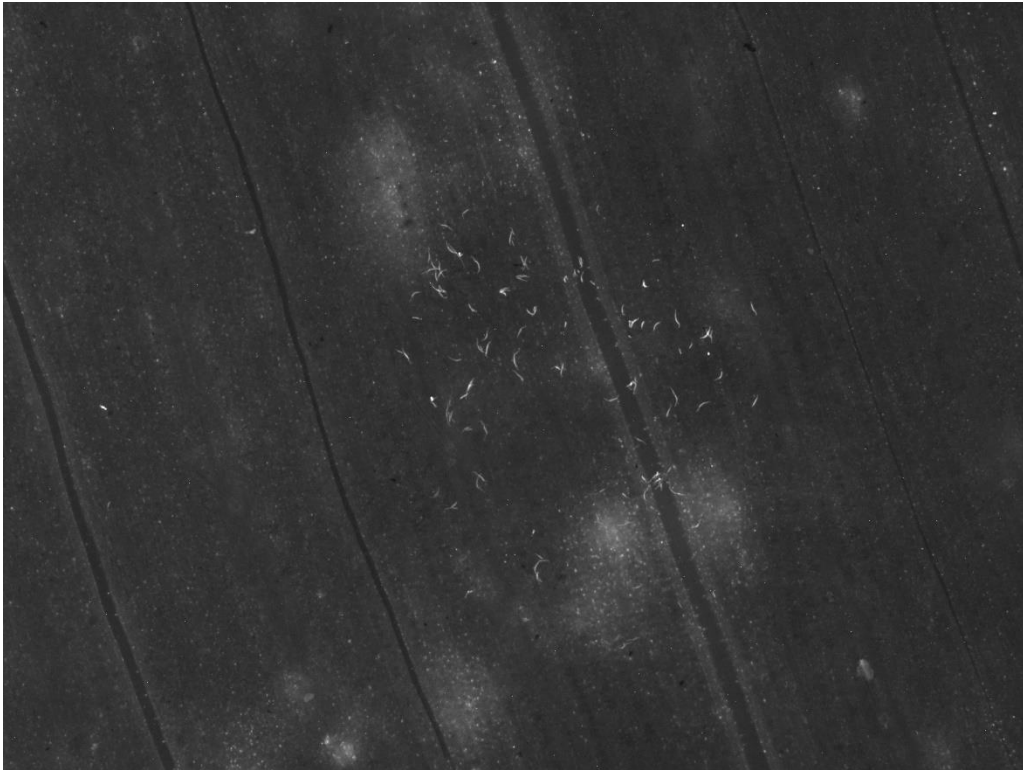
**Figure 3.4. GFP quantification of GFP-*C. heterostrophus* droplet infection sites.** Selected infection sites were excised with a 1 cm radius cork borer. Samples were homogenized, crude protein was extracted, and GFP fluorescence was measured with a 96-well plate reader. Greater fungal growth at 6 dpi was observed for *gl11* and *gl17* mutants. (A-B) Results shown on one genotype panel split in two experimental days. (C-D) Replicate experiments performed on assorted *glossy* mutants. Experiment was repeated four times, with three representative results shown. Statistics shown: Data is given as mean of 6 replicates  $\pm$  SE. Two-way ANOVA with Tukey's multiple comparisons. Indicated significance only show comparisons to wild-type W22; \*:  $p < 0.05$ , \*\*\*\*:  $p < 0.0001$ .

### **B. *C. heterostrophus* conidia have varying levels of adherence to leaf surfaces**

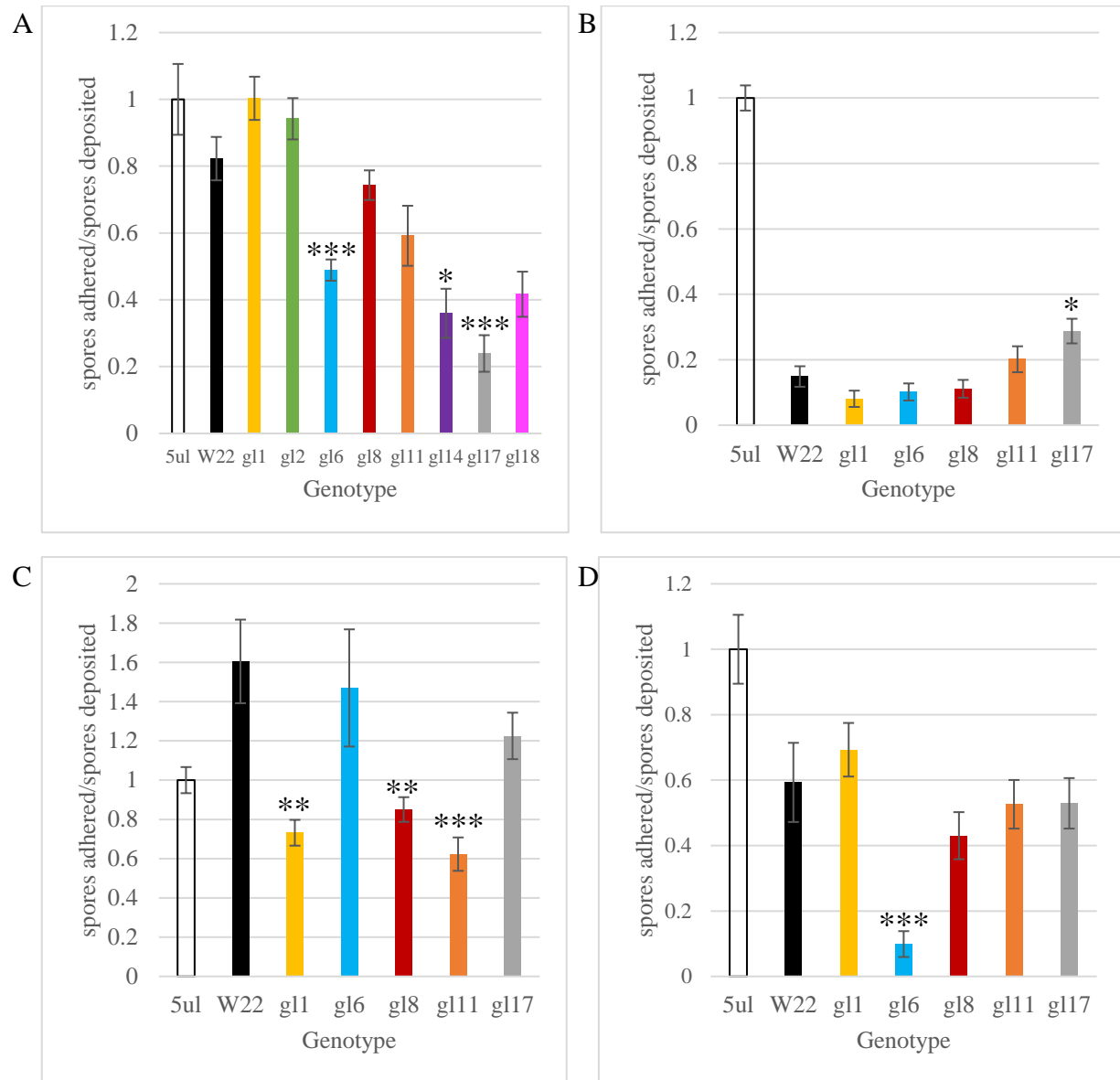
During initial stages of *C. heterostrophus* infection, conidia land on leaf surfaces and begin a rapid adhesion process by extracellular matrix production (Horwitz *et al.* 2013). Initial studies quantifying fungal attachment to artificial glass surfaces and juvenile maize leaves using liquid drip washing on slanted media support this claim (Braun and Howard 1994). Similarly, a previous study on another fungal pathogen investigated changes in *Blumeria graminis* conidia adherence on juvenile *gll1* mutants and they concluded that certain wax compounds can influence conidia adhesion and germination on leaf surfaces (Hansjakob *et al.* 2011). To investigate if adult maize cuticle can mediate early adherence stages of *C. heterostrophus* infection, and if higher susceptibility of *gll1* and *gll7* mutants to *C. heterostrophus* is caused by this process, we developed a fungal adhesion assay to fit our facilities. We used liquid baths at multiple time points post-droplet infection (1, 2, 3 hours) for our wash step and determined that two hours post-infection was sufficient for conidial adhesion (data not shown). With an established assay, we performed a series of adhesion assays on our *glossy* panel with 2-hour post-infection wash steps and visualized entire droplet infection sites at 200x magnification using an epifluorescence microscope with GFP fluorescence settings to quantify conidia on the leaf surface (Figure 3.5).

We began adhesion assays by manually counting the number of conidia found in a 5  $\mu$ l conidia suspension droplet as a measure of how many conidia were deposited on the leaf surface. We normalized each genotype's adhesion behavior as a ratio of total conidia deposited. After performing replicate adhesion assays, we found significant but no consistent changes in conidial adhesion across genotypes in all studies (Figure 3.6). In different experiments, *gll1* and *gll7* mutants showed significantly lower, higher, or no changes in adhesion rate compared to wild-type W22. This can be seen with the inconsistent behavior of *gll7*, which showed a 60% reduction in

adhesion rate compared to W22 in one experiment (Figure 3.6A), 50% increase in another (Figure 3.6B), and no significant change in others (Figure 3.6C, Figure 3.6D). Additionally, certain *glossy* genotypes (*gl1*, Figure 3.6C; *gl6*, Figure 3.6A, Figure 3.6D) with no significant differences in infection susceptibility showed varied significant changes in conidia adhesion rate. Therefore, we cannot make a conclusion about the adhesion rate behavior of *C. heterostrophus* on our genotype panel, or about the reliability of the adhesion assay on adult maize leaves.



**Figure 3.5. *C. heterostrophus* droplet infection site on maize leaf tissue visualized for adhesion assay quantification.** Infection site shown has 5  $\mu$ l of a  $2 \times 10^4$  *C. heterostrophus* conidia/ml suspension with a 2-hour post-infection wash step. Site was visualized with GFP fluorescence settings at 200x magnification, with optimal brightness, contrast and gain settings to distinguish conidia from leaf tissue and other debris.

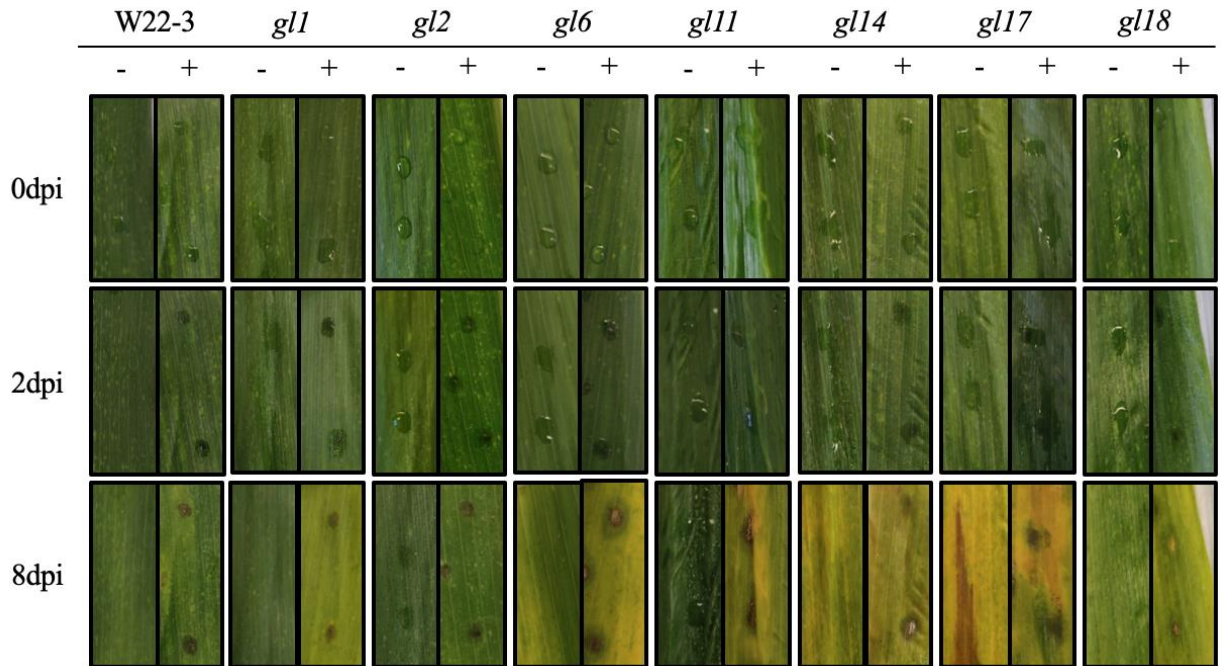


**Figure 3.6. *C. heterostrophus* conidia adherence rates to W22 and glossy mutant leaf surfaces.** (A-D) Droplet infections using 5  $\mu$ l droplets of a  $2 \times 10^4$  conidia/ml fungal solution with a 2-hour post-infection wash step was performed. Whole droplet infection sites were visualized at 200x magnification using GFP fluorescence settings on an epifluorescent microscope and attached conidia were quantified. Statistics shown: Data is given as mean of 24 replicates  $\pm$  SE. One-way ANOVA with Dunnett's multiple comparisons test. Indicated significance only show comparisons to wild-type W22; \*:  $p < 0.05$ , \*\*:  $p < 0.01$ , \*\*\*:  $p < 0.0002$ .

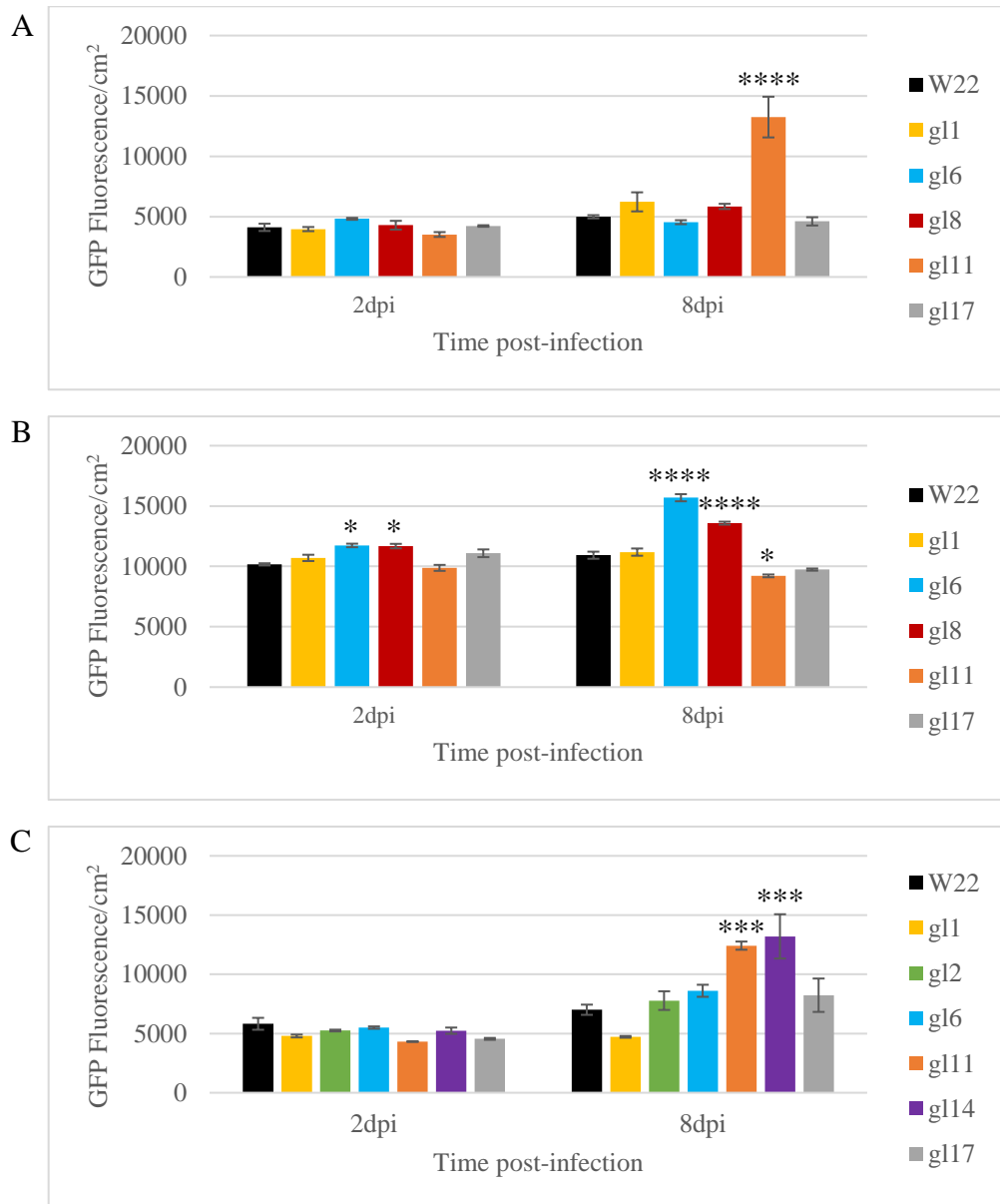
### ***C. gl11* mutants are more susceptible to *C. graminicola* infection**

Detached leaf infection assays using *C. graminicola* on juvenile maize and other grass varieties showed lesion formation at 4 dpi (Weihmann *et al.* 2016, Khan and Zhiang 2003). We were able to replicate their method on our *glossy* panel using juvenile leaves and subsequently modified it for testing on adult maize leaves (data not shown). During infection assay development, we did not observe large, dark lesions on detached leaves as shown in Figure 1.9A without encountering some problems 12 dpi: 1) fungal overgrowth of the leaf surface was observed and could have been caused by other environmental fungi, and 2) comparisons to mock-infected leaves showed that cell death symptoms could have been caused by leaf senescence in addition to our pathogen. Therefore, we modified our existing adult leaf pathogen assay to avoid these issues, allowing infections to continue for 8 dpi with quantification at 0, 2 and 8 dpi. We observed initial signs of tissue browning at 2dpi with small but distinct lesions at the droplet infection site at 8dpi (Figure 3.7).

We performed fungal growth quantification at 0, 2 and 8 dpi with the same protein extraction and GFP quantification method as described earlier. There was no significant difference across genotypes at 0 dpi (data not shown) or 2 dpi (Figure 3.8). Interestingly at 8 dpi, some *glossy* mutants showed significantly higher fungal loads (*gl6*, *gl8*, *gl14*; Figure 3.8B, Figure 3.8C), but only *gl11* showed consistently higher GFP quantity than other genotypes with at least double the amount of GFP compared to W22 with multiple replicate studies (Figure 3.8A, Figure 3.8C). Thus, we concluded that only *gl11* mutants were susceptible to *C. graminicola* infection. To summarize overall infection susceptibility of our *glossy* panel, *gl11* mutants showed higher susceptibility to both *C. heterostrophus* and *C. graminicola* infection, but *gl17* had no changes in susceptibility to *C. graminicola* compared to wild-type W22.



**Figure 3.7. Visual disease progression of W22 and *glossy* mutant detached leaves infected with *C. graminicola*.** 5  $\mu$ l droplet infection sites on detached adult leaf surfaces from the *glossy* panel were monitored over an 8-day time course. (-): Mock infection with 5  $\mu$ l droplets of sterile 0.05% Tween 20. (+): Infection with 5  $\mu$ l droplets of  $1 \times 10^6$  *C. graminicola* conidia/ml in 0.05% Tween 20. Panel shows results from one infection performed on the largest *glossy* panel, and three other experiments follow the same trend. Initial lesion formation is observed 2 dpi, with varying levels of lesion formation at 8 dpi. 0 dpi infection photos for *glossy* mutants are not shown, as all leaves show the same visual behavior as wild-type W22. Experiments were repeated four times, with representative results shown.



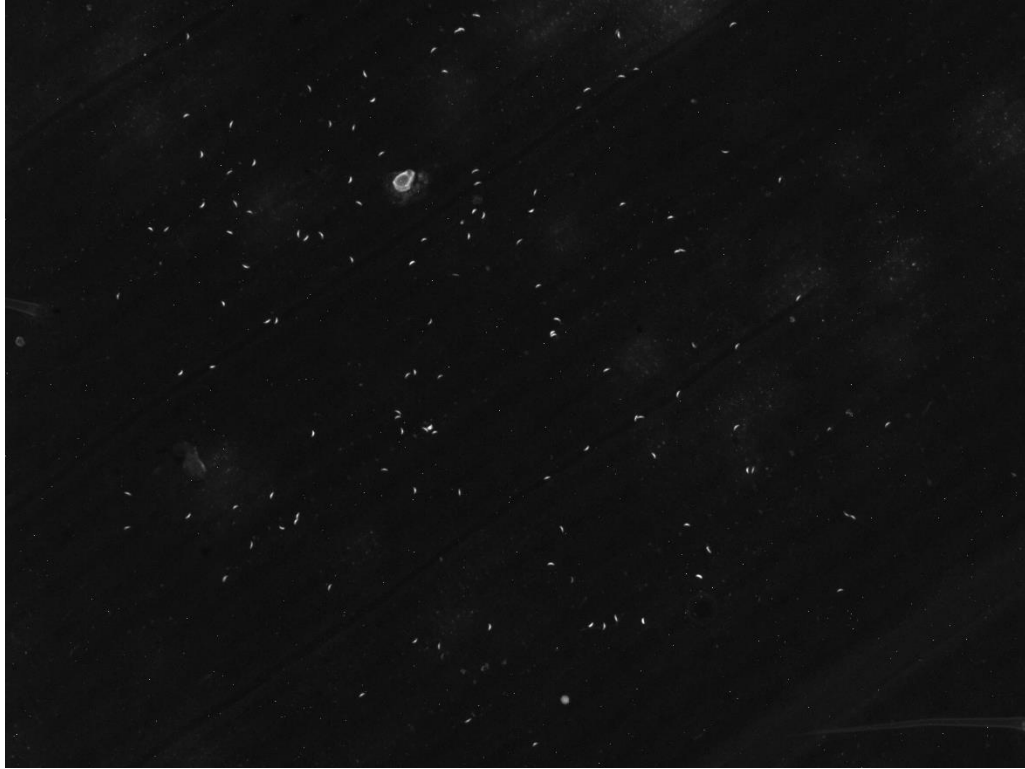
**Figure 3.8. Quantification of GFP-*C. graminicola* droplet infection sites.** Selected infection sites were excised with a 1 cm radius cork borer. Samples were homogenized, crude protein was extracted, and GFP fluorescence was measured with a 96-well plate reader. Greater fungal growth at 8 dpi was observed for *gl11* mutants. (A-C) Experiments were repeated four times, with three representative results shown. Statistics shown: Data is given as mean of 6 replicates  $\pm$  SE. Two-way ANOVA with Tukey's multiple comparisons. Indicated significance only show comparisons to wild-type W22; \*:  $p < 0.05$ , \*\*\*:  $p < 0.0002$ , \*\*\*\*:  $p < 0.0001$ .

#### **D. *C. graminicola* conidia have varying levels of adherence to leaf surfaces**

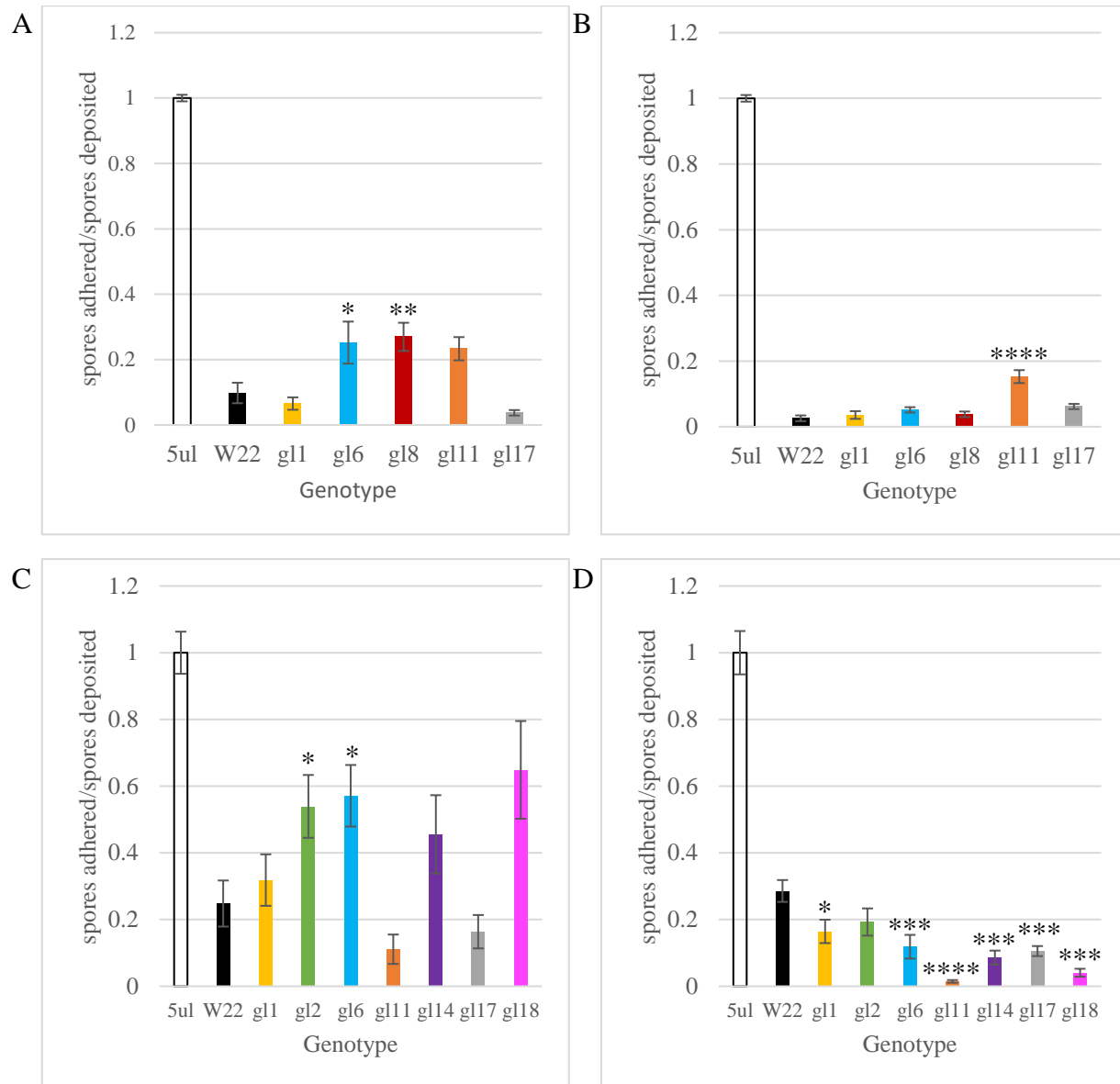
During early *C. graminicola* infection, conidia will germinate and form appressoria upon recognition of the cuticle. Prior studies on *C. graminicola* adhesion to adult maize indicate adhesion and appressorium formation are necessary for infection progression (Mercure *et al.* 1994, Weihmann *et al.* 2016). Similar to our *C. heterostrophus* infection assays, we investigated adult maize cuticle's role in early adherence stages of *C. graminicola* infection, and if higher susceptibility of *gll1* mutants to *C. graminicola* is caused by this process. We modified our existing fungal adherence assay for *C. graminicola* infections and determined the optimal wash step for sufficient adhesion time was 4 hpi (data not shown). We visualized whole droplet infection sites using the same epifluorescent microscopy settings for *C. heterostrophus* adhesion assays and quantified adherent conidia by observing fluorescent signals from attached conidia (Figure 3.9).

We observed similar inconsistencies in adhesion rate significance across our *glossy* panel as our *C. heterostrophus* adhesion assays (Figure 3.10). Susceptible *gll1* mutants showed variable behavior, where they show four-fold increase in conidia adhesion in one replicate (Figure 3.10B), a total lack of adhesion in another (Figure 3.10D), or no change in adhesion compared to W22 (Figure 3.10A, Figure 3.10C). Because *gll1* mutants do not have consistent conidial adhesion rates across multiple experiments and most other *glossy* mutants with no change in infection susceptibility showed differences in adhesion rate (*gll1*, *gl2*, *gl6*, *gl8*, *gl14*, *gl17*, *gl18*; Figure 3.10A, Figure 3.10C, Figure 3.10D), we cannot make a conclusion about adhesion rate changes of *C. graminicola* on our genotype panel, or the reliability of this adhesion assay either.





**Figure 3.9. *C. graminicola* droplet infection site on maize leaf tissue visualized for adhesion assay quantification.** Infection site shown has 5  $\mu\text{l}$  of a  $2 \times 10^4$  *C. graminicola* conidia/ml suspension with a 2-hour post-infection wash step. Site was visualized with GFP fluorescence settings at 200x magnification, with optimal brightness, contrast and gain settings to distinguish conidia from leaf tissue and other debris.



**Figure 3.10. *C. graminicola* conidia adherence rates to W22 and glossy mutant leaf surfaces.** (A-D) Droplet infections using 5  $\mu$ l droplets of a  $2 \times 10^4$  conidia/ml fungal solution with a 2-hour post-infection wash step was performed. Whole droplet infection sites were visualized at 200x magnification using GFP fluorescence settings on an epifluorescent microscope and attached conidia were quantified. Statistics shown: Data is given as mean of 24 replicates  $\pm$  SE. One-way ANOVA with Dunnett's multiple comparisons test. Indicated significance only show comparisons to wild-type W22; \*:  $p < 0.05$ , \*\*:  $p < 0.01$ , \*\*\*:  $p < 0.0002$ .

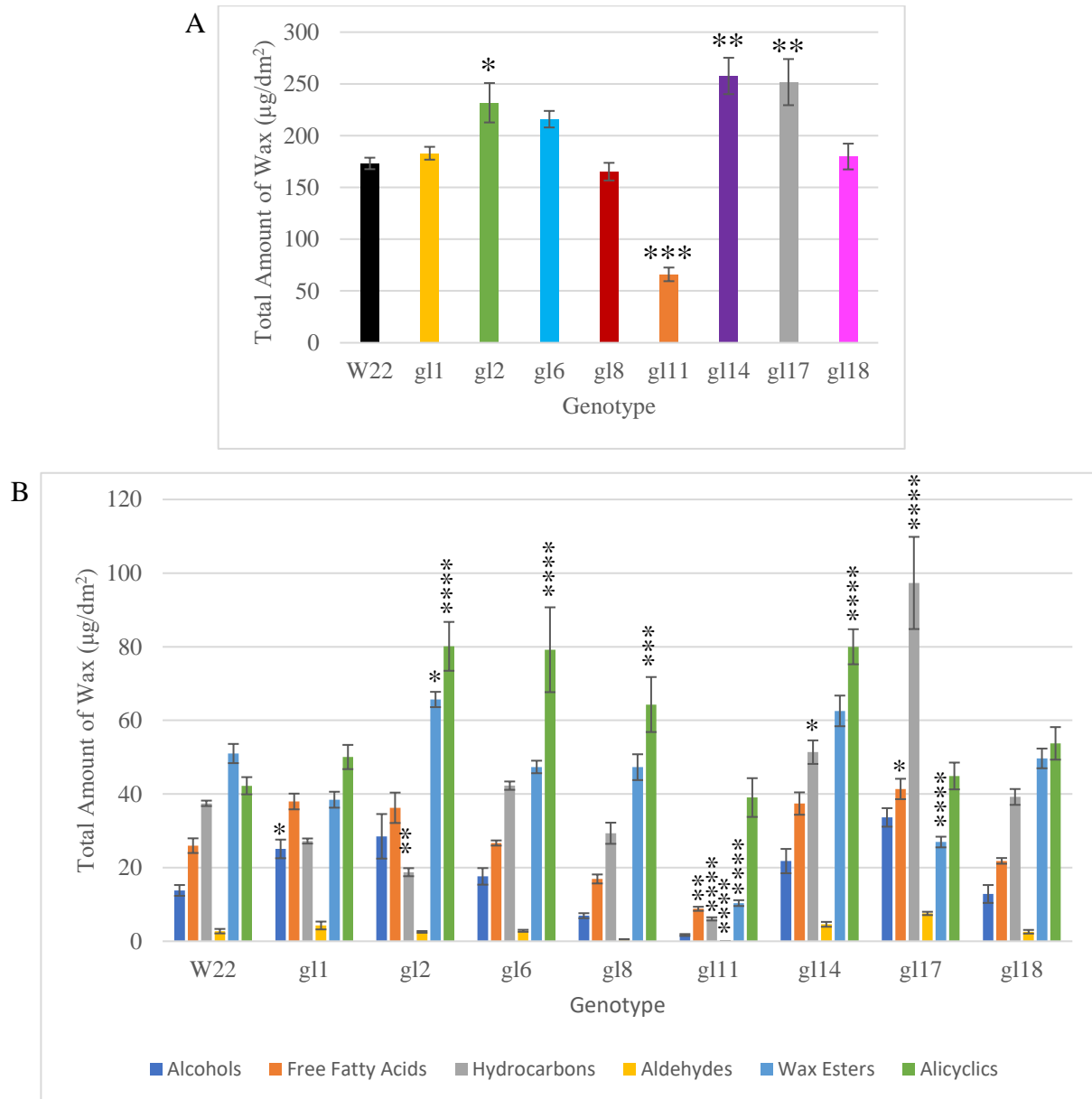
## **E. Adult *gl11* and *gl17* mutant cuticles have altered wax profiles compared to wild-type W22**

We formally acknowledge Dr. Richard Bourgault and Dr. Isabel Molina (Algoma University, Canada) for performing cuticle wax extraction and GC/MS analysis on our *glossy* panel.

We observed the cuticle defect phenotype on our genotype panel by performing the water adherence phenotype screen on juvenile plants. RNA expression data on different stages of maize development indicates that some of the known *glossy* genes that play a role in cuticle wax biosynthesis are actively expressed during adult stage (Figure 1.6, Sekhon *et al.* 2011). Therefore, we hypothesized that we would also observe cuticle composition differences on our adult *glossy* panel, which may provide insight on what cuticle components may influence pathogen resistance. Ongoing studies related to this project by other collaborators have established adult maize cuticle ultrastructure, wax composition, and other phenotypes (Figure 1.1, other unpublished lab data not shown). For our cuticle wax analysis, we used adult leaves of comparable developmental stage on our *glossy* panel. An entire adult leaf with its sheath covering the uppermost developed ear on the maize plant was cut off the plant, and an intact, 14-15 cm in length portion of the middle leaf section excised for wax extraction.

The two genotypes, *gl11* and *gl17*, which show changes in infection susceptibility, also show differences in overall wax load and individual wax components compared to W22. Adult *gl11* mutants have less than half the total wax load compared to adult W22 (Figure 3.11A). When examining the individual wax classes, *gl11* mutants show major reductions in free fatty acid, hydrocarbon and wax ester content by up to 70%, and no significant differences in alcohol, aldehyde or alicyclic content (Figure 3.11B). Adult *gl2*, *gl14*, and *gl17* mutants all have a significantly higher wax load compared to adult W22 by over 30% (Figure 3.11A). *gl17* mutants

show a significantly higher free fatty acid and hydrocarbon content by at least 25% and 50% respectively but have significantly reduced wax ester content by 50% (Figure 3.11B). Because *g111* and *g117* mutants have changes in infection susceptibility to our pathogens and have significantly lower and higher wax loads respectively, we conclude that total wax amount is not the primary driving force of infection susceptibility to both pathogens.

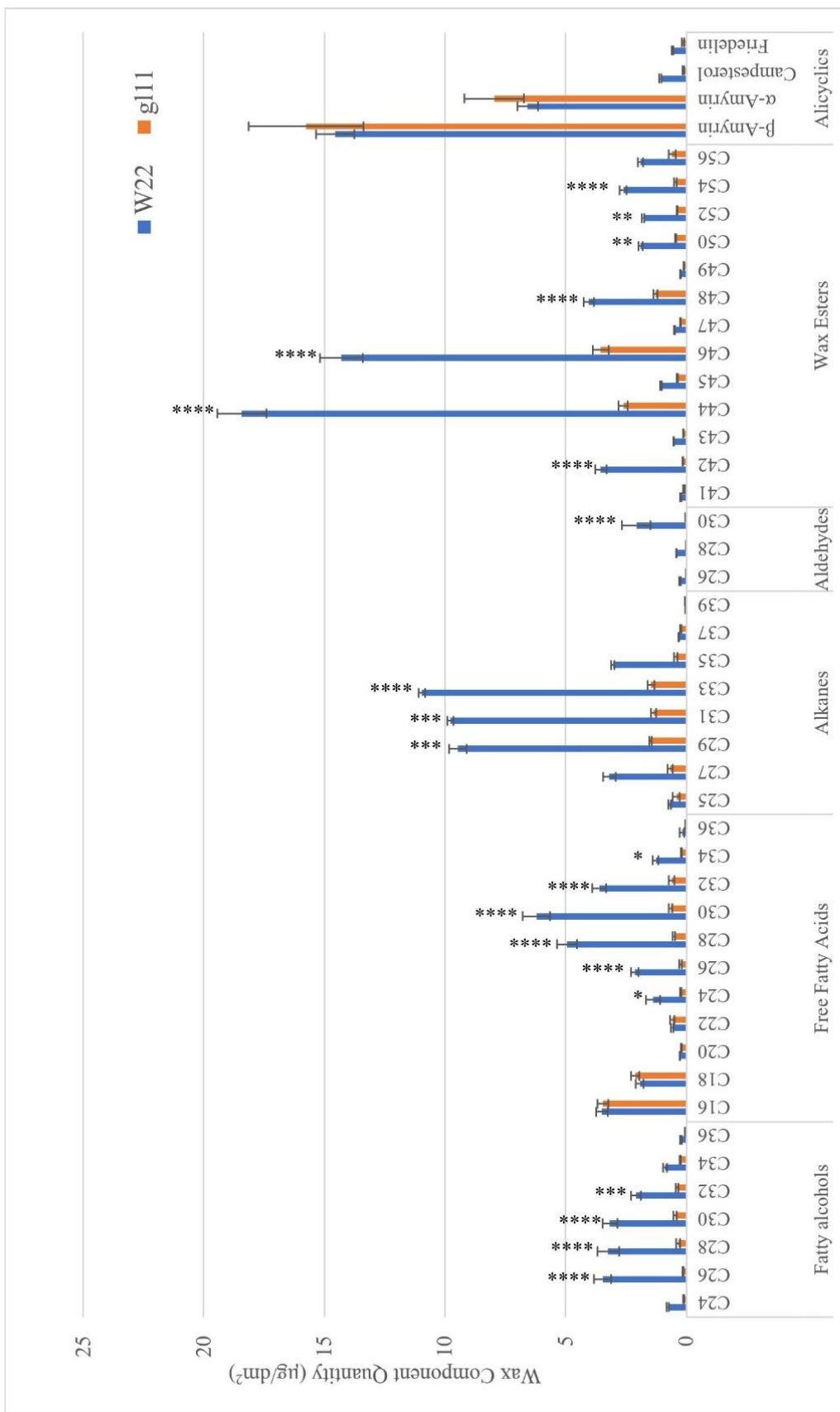


**Figure 3.11. Overall total cuticle wax load and wax classes of W22 and glossy mutants. (A)** Total cuticle wax load of genotype panel. Statistics shown: Data is given as mean of 3 replicates  $\pm$  SE. One-way ANOVA with Dunnett's multiple comparisons test. **(B)** Individual cuticle wax class loads of genotype panel. Statistics shown: Data is given as mean of 3 replicates  $\pm$  SE. Two-way ANOVA with Dunnett's multiple comparisons test. Indicated significance only show comparisons to wild-type W22; \*,  $p < 0.05$ , \*\*,  $p < 0.01$ , \*\*\*,  $p < 0.0002$ , \*\*\*\*,  $p < 0.0001$ .

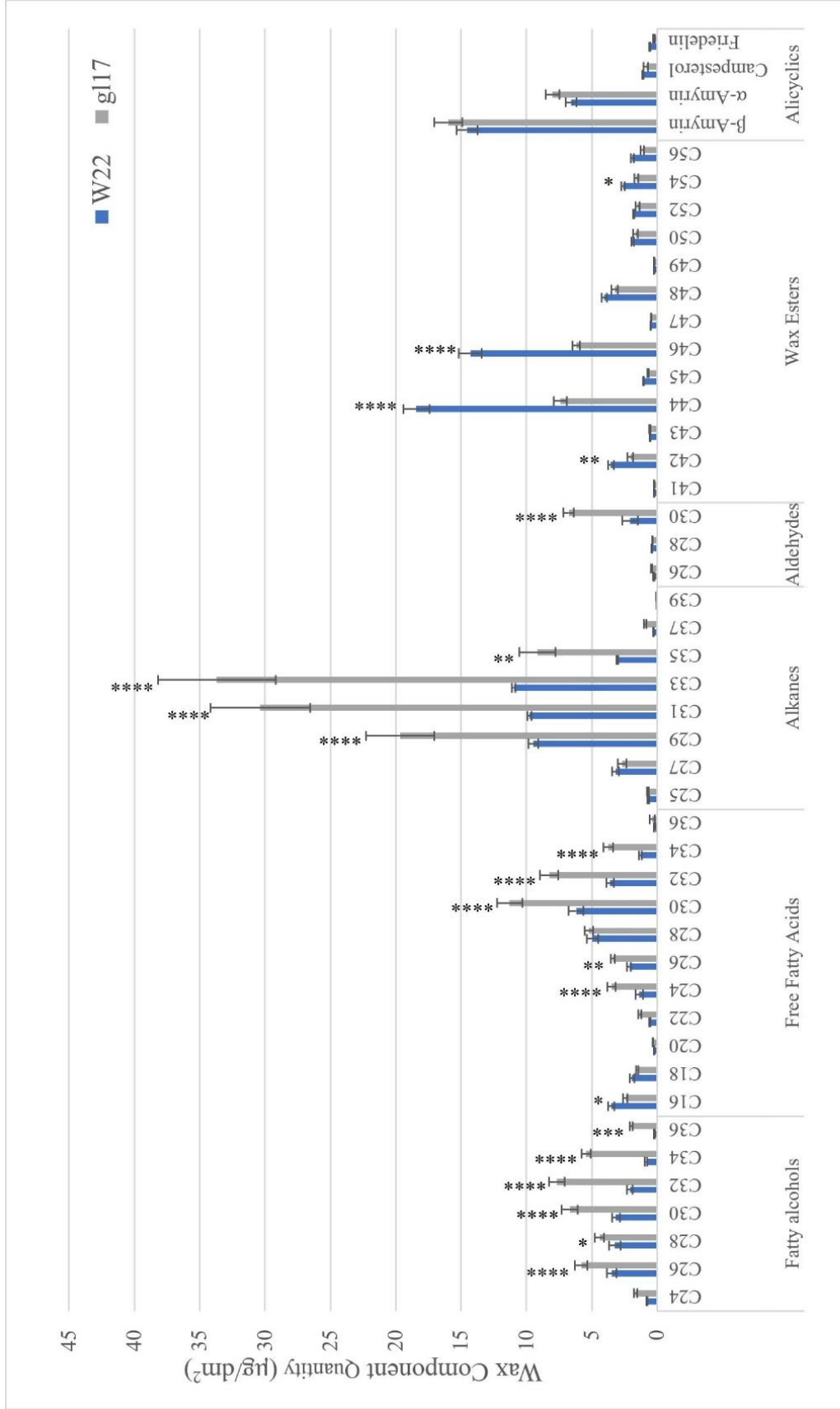
Because *gll1* mutants showed significant deficiencies in total wax load and individual wax classes, we expected to observe overall decreases in many individual wax constituent profiles of each wax class. *gll1* mutants showed nearly depleted levels of C26-32 fatty alcohols, C24-32 free fatty acids, C29-33 alkanes, C30 aldehydes, and about 18% of even-numbered lengths of C42-54 wax esters compared to W22 (Figure 3.12). However, we noted that there were no significant changes in C16-C22 free fatty acids and certain alicyclic compounds ( $\beta$ -Amyrin and  $\alpha$ -Amyrin). This indicates that these particular compounds are accumulated at a higher percentage of the overall *gll1* total wax profile compared to wild-type.

We expected to see similar changes in individual wax constituent profiles in *gll7* mutants as their wax classes. We observed a minimum increase of 25% in C26-36 fatty alcohols, a 50% increase in C24-26 and C30-34 free fatty acids, at least a two-fold increase in C29-35 alkanes and C30 aldehydes. However, the C42-46 and C54 wax esters showed a two-fold, significant reduction (Figure 3.13).

The two susceptible genotypes, *gll1* and *gll7*, both share an overall reduction in wax ester content, particularly with the C42-46 and C54 lengths. By comparison, wax esters have the highest concentration of individual wax constituents in cuticles in adult W22 (Figure 3.11) and in adult B73 (Figure 1.1C). We propose that wax esters at those chain lengths may play a role in providing pathogen defense, but we cannot make this conclusion without further experimentation.



**Figure 3.12. Individual cuticle wax constituents organized by carbon chain length in adult wild-type W22 and g111 mutants.** Statistics shown: Data is given as mean of 3 replicates ± SE. Two-way ANOVA with Dunnett's multiple comparisons test. Indicated significance shows comparison to W22; \*, p < 0.05, \*\*, p < 0.01, \*\*\*, p < 0.0002; \*\*\*\*, p < 0.0001.



**Figure 3.13. Individual cuticle wax constituents organized by carbon chain length in adult wild-type W22 and *gl17* mutants.** Statistics shown: Data is given as mean of 3 replicates ± SE. Two-way ANOVA with Dunnett's multiple comparisons test. Indicated significance shows comparison to W22; \*,  $p < 0.05$ , \*\*,  $p < 0.01$ , \*\*\*,  $p < 0.0002$ ; \*\*\*\*,  $p < 0.0001$ .



## CHAPTER 4: Discussion

In this study, we investigated the role of adult maize cuticle in providing resistance to *C. heterostrophus* and *C. graminicola* using a forward genetics approach with maize *glossy* cuticle mutants where some of them (*gl11*, *gl17*) show changes in infection susceptibility. We established fungal disease susceptibility on an adult *glossy* mutant panel and investigated cuticle-related phenotypes and behavior that may contribute to this phenotype. Our initial testing period to establish a method to quantify fungal disease infection susceptibility involved replicating infection results from previously described literature and we observed clear lesion formation on juvenile wild-type W22 leaves against *C. heterostrophus* and *C. graminicola* similar to their studies (Figure 3.2, Degani *et al.* 2014, Weihmann *et al.* 2016). We modified their existing method for these pathogens on adult leaves because infection behavior was slightly different compared to pathogenicity on juvenile leaves. While juvenile leaves showed clear lesion formation as early as 1 dpi for both *C. heterostrophus* and *C. graminicola*, we only observed small, yet distinguishable lesions at 1 dpi (*C. heterostrophus*) and 2 dpi (*C. graminicola*) on adult leaves; therefore, we allowed our infections to progress for longer periods of time to observe distinguishable lesions comparable to the juvenile leaf studies described by others (Figure 3.2, Figure 3.3, Figure 3.7). We used protein extraction with GFP fluorescence to quantify our infection susceptibility because this observation implied that there was fungal growth at the infection site after 6 dpi (*C. heterostrophus*) or 8 dpi (*C. graminicola*). Overall, we consistently found that *gl11* mutants were more susceptible to both *C. heterostrophus* and *C. graminicola*, whereas *gl17* mutants were susceptible only to *C. heterostrophus* (Figure 3.4, Figure 3.8). With this method, we did not observe significant differences between 0 dpi and 1 dpi (*C. heterostrophus*) or 2 dpi (*C. graminicola*), our first quantification time points (data not shown). One method to track sensitive

changes in fungal growth at the earlier infection time points or consistently distinguish genotype susceptibility at later stages would be to perform a qPCR on fungal DNA for both pathogen assays (Weihmann *et al.* 2016). This method would also provide clearer data for lines in which infection susceptibility was unclear (*gl1*, *gl2* and *gl6*, Figure 3.4A, Figure 3.4D; *gl6*, *gl8* and *gl14*, Figure 3.7, Figure 3.8B, Figure 3.8C). Additionally, *C. graminicola* infection on juvenile maize has shown to be more effective during low-light conditions and would be an effective area to investigate (Schall *et al.* 1980).

To explore potential explanations for changes in infection susceptibility, we first examined changes in fungal adherence to *glossy* leaf surfaces. After developing adhesion assays for *C. heterostrophus*, we found that conidial adherence of both pathogens on leaf surface was largely inconsistent—many genotypes with no susceptibility phenotype showed inconsistent and significant changes in adhesion rates (Figure 3.6). The more susceptible mutants, *gl11* and *gl17*, did not show consistently increased adhesion rates of *C. heterostrophus*—thus, changes in conidial adherence do not provide an explanation for increased susceptibility to this pathogen. Additionally, some of the *glossy* mutants without a pathogen susceptibility phenotype showed inconsistent and significant differences in fungal adhesion rates against *C. heterostrophus*, which further attests to the unreliability of this adhesion assay on adult maize leaves. This trend was also true for *C. graminicola* infection. *gl11*, the only susceptible *glossy* mutant to *C. graminicola* infection, shows inconsistent conidia adherence rates, and mutants with no susceptibility phenotype show changes in adherence (Figure 3.9). Therefore, changes in *C. graminicola* adherence do not explain susceptibility to *C. graminicola* either. Although we do not know why *gl11* and *gl17* mutants show different behavior when exposed to both pathogens, they must have different biological

explanations for their susceptibility phenotype, because *gll1* is susceptible to both *C. heterostrophus* and *C. graminicola*, whereas *gll7* is only susceptible to *C. heterostrophus*.

Interestingly, a cuticle-pathogen relationship study on *Blumeria graminis* conidial pre-penetration events on *gll1* mutant leaves included similar experiments as our study, and they concluded that the reduction of VLCFAs inhibited *B. graminis* conidia germination on *gll1* leaf surfaces (Hansjakob 2011). Unfortunately, they did not relate their adhesion study to infection susceptibility to this pathogen, and we can only speculate that a reduction in *B. graminis* conidia adherence to the *gll1* leaf surface would result in increased resistance to this pathogen. In the same study, they observed changes in conidial adhesion and germination using artificial glass slides coated with cuticular wax extracts and juvenile detached maize leaves and related them to *gll1*'s known aldehyde deficiency (Avato *et al.* 1985). Our adult *gll1* mutants showed a total wax deficiency similar to juvenile leaves used in their study, but do not show the same increased wax ester or alcohol content (Figure 3.11). This observation corroborates claims from other literature that show cuticle composition differences in the same plant species in different developmental stages (Jenks and Ashworth 2010). To further explore the role of cuticular wax composition against conidia adherence, we could perform adhesion assays or check germination rates for both *C. heterostrophus* and *C. graminicola* adhesion *in vitro* on glass slides using artificially created wax profiles or extracted cuticle waxes from leaves. While these experiments do not show the behavior of conidia on leaves, it may provide insight as what cuticle waxes may influence conidia pre-penetration events (Hansjakob 2011, Braun and Howard 1994).

We wanted to observe and quantify early penetration of both pathogens using fluorescent staining and confocal microscopy, as their infection mechanisms involve direct entry through the cuticle and some studies indicate that certain cuticle waxes may induce appressorium formation

for a fungal infection's adhesion and penetration process (Gilbert *et al.* 1996). A previous study relating greater cuticle permeability and low cuticle thickness with enhanced *C. heterostrophus* growth and may provide insight for *gll1*'s susceptibility phenotype in relation to fungal penetration (Lequeu *et al.* 2003). Additionally, disruption of wax recognition mechanisms can lead to reduced pathogenicity of certain fungi, like *Colletotrichum gloeosporoides* (Hwang *et al.* 1995). Method establishment to determine the maize cuticle's role in regulating fungal penetration is currently ongoing. Using a modified propidium iodide and wheat germ agglutinin stain, we observed penetration of *C. heterostrophus* on adult W22 leaves during our initial trial assays (data not shown) but quantification attempts have been unsuccessful so far. Other quantitative fungal penetration studies using different pathogens like *C. graminicola* on juvenile maize or *Colletotrichum acutatum* on almond tissue provide a direction for our study (Weihmann *et al.* 2016, Dieguez-Uribeondo *et al.* 2005). The presence of internal light spots on *C. acutatum* appressoria indicate sites of penetration through almond leaf epidermal tissue, which may provide an effective means in quantifying penetration using *C. graminicola* on our *glossy* mutant panel (Dieguez-Uribeondo *et al.* 2005). Further testing with *C. graminicola* penetration is currently ongoing using a modified *C. graminicola* infection, fixation and staining assay based on their findings.

In our cuticle wax composition analysis, we found that adult *gll1* mutants have significantly decreased overall wax load, and major reductions in most major wax classes, including fatty alcohols, fatty acids, alkanes, aldehydes and wax esters (Figure 3.11). Current studies in our lab to identify and clone *gll1* and *gll7* will aid in identifying their gene functions in relation to our observed cuticle wax composition phenotypes. The *gll1* gene is still unknown but has been mapped to chromosome 2 in between *bngl125* and *umc34* loci using QTL analysis

(Neuffer *et al.* 1997, Krakowsky 2006). The wax profile of *gl11* has only been studied in juvenile maize and shows differences with our results on adult *gl11* (Hansjakob *et al.* 2011). In their study, they observed no changes in alcohol content, slightly elevated relative alkane and wax ester load, and major deficiency in aldehyde content in juvenile *gl11* compared to juvenile C836B and Lambda maize lines, which contrasts our comparison in adult *gl11* against W22. Because most wax compounds are deficient in *gl11*, we propose that its gene function lies upstream in cuticle biosynthesis pathway in the Fatty Acid Elongase (FAE) complex (Figure 1.3). *Arabidopsis thaliana* mutants (*cer6*, *cer10*, *pas2*, *kcr1*) with defects in the FAE complex show dramatic aliphatic wax decreases in all wax classes and have growth defects, similar to *gl11* (Figure 3.12, Figure 3.1, Shumborski *et al.* 2016, Zheng *et al.* 2005, Bach *et al.* 2008, Beaudoin *et al.* 2009). This hypothesis can be explored further with BLAST, or DNA sequence analysis with a cloned *gl11* gene to existing FAE/LACS *Arabidopsis thaliana* models, and by confirming those models' susceptibility to pathogen attack.

The *gl17* gene is unknown but has been mapped to chromosome 5 (Neuffer *et al.* 1997). Primary literature on maize *gl17* is limited to its description and QTL mapping—to our knowledge, this is the first cuticular wax analysis on this mutant. Adult *gl17* mutants show a similar cuticle composition as *Arabidopsis thaliana* *wsd1* mutants, which encodes for a wax ester synthase/diacylglycerol acyltransferase that synthesizes wax esters from free fatty alcohols and free fatty acids (Figure 1.3, Figure 3.13, Li *et al.* 2008). Most notably, both *gl17* and *wsd1* mutants have increased primary alcohol content (C26-30) and reduced (*gl17*) or lack of (*wsd1*) wax esters (C40-44). In contrast, our *gl17* mutant showed an increased overall alkane and free fatty acid content that is not shown in *wsd1* mutants. Biochemical pathways for *wsd1* indicate that one of its functions involves synthesizing wax esters from free fatty acids and fatty alcohols (Figure 1.3)

Therefore, we propose that *gl17* has a similar function to *wsd1* in *Arabidopsis thaliana*, because decreased *wsd1* function would lead to an accumulation of both free fatty alcohols and free fatty acids as shown in both maize *gl17* mutants and *Arabidopsis thaliana wsd1* mutants. Notably, *gl17* mutants do not show a complete knockdown of wax ester load that is seen in *wsd1* mutants from their study. We propose two explanations for this: 1) *gl17* mutants have decreased gene function that significantly impairs wax ester production but does not completely eliminate it, or 2) *gl17* has redundant gene function, so wax ester production is impaired but not totally depleted. Similar to *gl11*, this proposal can be explored with BLAST, or DNA sequence analysis of a cloned *gl17* gene to *wsd1* and with pathogen infection assays on *wsd1* mutants.

## Conclusion and Outlook

In our study, we found that *gl11* mutants are more susceptible to both *C. heterostrophus* and *C. graminicola*, and *gl17* mutants are more susceptible only to *C. heterostrophus*. We identified changes in cuticle composition for both mutants and established that changes in infection susceptibility are not correlated with fungal adhesion to cuticle for both pathogens; we hope to explore differences in fungal penetration as a potential explanation for increased fungal pathogenicity on our *glossy* panel. To our knowledge, this is a novel study that characterizes the adult maize cuticle in relation to pathogen resistance using cuticle *glossy* mutants. Current studies ongoing in the Smith research group related to this study include the cloning of *gl11* and *gl17* by other members of the research group and testing our *glossy* genotype panel's resistance behavior to *C. heterostrophus* under field-grown conditions with the help of Dr. Peter Balint-Kurti at North Carolina State University.

Although many of our mutants did not show a change in their pathogen resistance, there are other agronomically important phenotypes to explore. In a related study, we performed a leaf cuticular dehydration analysis and found that adult *gl6*, *gl8*, *gl11*, and *gl14* mutants had showed changes in water loss rate through the cuticle barrier compared to wild-type W22 (results not shown). Other collaborators are investigating the natural variation in maize across the maize Wisconsin Diversity Panel (WiDiv) and are performing maize genome- and transcriptome-wide associated studies to identify the genetic control of this behavior. Functional analysis to determine the genetic basis for adult maize cuticle's role in drought tolerance is ongoing by collaborators. Additionally, transmission electron microscopy analysis methods previously performed on B73 (Figure 1.1B) is currently being applied to our *glossy* panel and the WiDiv panel, and we hope to see changes in our *glossy* mutants' cuticle ultrastructure compared to W22.

## CHAPTER 5: References

- Anderson, B. “Fungi Associated with Cornstalks in Illinois in 1982 and 1983.” *Plant Disease*, vol. 71, no. 2, 1987, p. 135., doi:10.1094/pd-71-0135.
- “Anthracnose Stalk Rot.” *Anthracnose Stalk Rot*, DuPont Pioneer, 2013, www.pioneer.com/home/site/us/agronomy/crop-management/corn-insect-disease/anthracnose-stalk-rot/#Facts.
- Apoga, Dace, John Barnard, Harold G. Craighead, and Harvey C. Hoch. “Quantification of Substratum Contact Required for Initiation of *Colletotrichum graminicola* Appressoria.” *Fungal Genetics and Biology*, vol. 41, no. 1, 2004, pp. 1–12., doi:10.1016/j.fgb.2003.10.001.
- Aragón, Wendy, José Juan Reina-Pinto, and Mario Serrano. “The Intimate Talk Between Plants and Microorganisms at the Leaf Surface.” *Journal of Experimental Botany*, vol. 68, no. 19, 2017, pp. 5339–5350., doi:10.1093/jxb/erx327.
- Bach, Liên, Louise V. Michaelson, Richard Haslam, Yannick Bellec, Lionel Gissot, Jessica Marion, Marco Da Costa, Jean-Pierre Boutin, Martine Miquel, Frederique Tellier, Frederic Domergue, Jonathan E. Markham, Frédéric Beaudoin, Johnathan A. Napier, and Jean-Denis Faure. “The Very-Long-Chain Hydroxy Fatty Acyl-CoA Dehydratase PASTICCINO2 Is Essential and Limiting for Plant Development.” *Proceedings of the National Academy of Sciences*, vol. 105, no. 38, 2008, pp. 14727–14731., doi:10.1073/pnas.0805089105.
- Beaudoin, Frédéric, Xianzhong Wu, Fengling Li, Richard P. Haslam, Jonathan E. Markham, Huanquan Zheng, Jonathan A. Napier, and Ljerka Kunst. “Functional Characterization of the Arabidopsis  $\beta$ -Ketoacyl-Coenzyme A Reductase Candidates of the Fatty Acid Elongase.” *Plant Physiology*, vol. 150, no. 3, 2009, pp. 1174–1191., doi:10.1104/pp.109.137497.
- Bergstrom, Gary C., and Ralph L. Nicholson. “The Biology of Corn Anthracnose: Knowledge to Exploit for Improved Management.” *Plant Disease*, vol. 83, no. 7, 1999, pp. 596–608., doi:10.1094/pdis.1999.83.7.596.
- Boller, Thomas, and Georg Felix. “A Renaissance of Elicitors: Perception of Microbe-Associated Molecular Patterns and Danger Signals by Pattern-Recognition Receptors.” *Annual Review of Plant Biology*, vol. 60, no. 1, 2009, pp. 379–406., doi:10.1146/annurev.arplant.57.032905.105346.
- Bourgault, Richard, Susanne Matschi, Miguel Vasquez, Pengfei Qiao, Annika Sonntag, Caleb Charlebois, Marc Mohammadi, Michael J. Scanlon, Laurie G. Smith, and Isabel Molina. “Changes in Lipid Composition and Ultrastructure Associated with Functional Maturation of the Cuticle during Adult Maize Leaf Development.” 2019, doi: 10.1101/625343.



- Braun, Edward J., and Richard J. Howard. "Adhesion of *Cochliobolus heterostrophus* Conidia and Germlings to Leaves and Artificial Surfaces." *Experimental Mycology*, vol. 18, no. 3, 1994, pp. 211–220., doi:10.1006/emyc.1994.1021.
- Bruns, H. Arnold. "Southern Corn Leaf Blight: A Story Worth Retelling." *Agronomy Journal*, vol. 109, no. 4, 2017, p. 1218., doi:10.2134/agronj2017.01.0006.
- Burch, Adrien Y., Briana K. Shimada, Sean W. A. Mullin, Christopher A. Dunlap, Michael J. Bowman, and Steven E. Lindow. "*Pseudomonas syringae* Coordinates Production of a Motility-Enabling Surfactant with Flagellar Assembly." *Journal of Bacteriology*, vol. 194, no. 6, 2011, pp. 1287–1298., doi:10.1128/jb.06058-11.
- Carson, M. L. "Compendium of Corn Diseases, Fourth Edition." *Foliar Diseases*, 2016, doi:10.1094/9780890544945.
- Carver, Timothy L. W., Hitoshi Kunoh, Barry J. Thomas, and Ralph L. Nicholson. "Release and Visualization of the Extracellular Matrix of Conidia of *Blumeria graminis*." *Mycological Research*, vol. 103, no. 5, 1999, pp. 547–560., doi:10.1017/s0953756298007400.
- Degani, Ofir. "Pathogenicity Assay for *Cochliobolus heterostrophus* G-Protein and MAPK Signaling Deficiency Strains." *American Journal of Plant Sciences*, vol. 05, no. 09, 2 Apr. 2014, pp. 1318–1328., doi:10.4236/ajps.2014.59145.
- Deising, Holger B., Stefan Werner, and Marcus Wernitz. "The Role of Fungal Appressoria in Plant Infection." *Microbes and Infection*, vol. 2, no. 13, 2000, pp. 1631–1641., doi:10.1016/s1286-4579(00)01319-8.
- Dietrich, Charles R., M. Ann D. N. Perera, Marna D. Yandean-Nelson, Robert B. Meeley, Basil J. Nikolau, and Patrick S. Schnable. "Characterization of Two *GL8* Paralogs Reveals That the 3-Ketoacyl Reductase Component of Fatty Acid Elongase Is Essential for Maize (*Zea mays* L.) Development." *The Plant Journal*, vol. 42, no. 6, 2005, pp. 844–861., doi:10.1111/j.1365-313x.2005.02418.x.
- Diéguez-Uribeondo, J., H. Förster, A. Soto-Estrada, and Jim E. Adaskaveg. "Subcuticular-Intracellular Hemibiotrophic and Intercellular Necrotrophic Development of *Colletotrichum acutatum* on Almond." *Phytopathology*, vol. 95, no. 7, 2005, pp. 751–758., doi:10.1094/phyto-95-0751.
- Doehlemann, Gunther, Patrick Berndt, and Matthias Hahn. "Different Signalling Pathways Involving a G $\alpha$  protein, cAMP and a MAP Kinase control germination of *Botrytis cinerea* conidia." *Molecular Microbiology*, vol. 59, no. 3, 2006, pp.821-835., doi:10.1111/j.1365-2958.2005.04991.x.
- Fan, Li. "Map Based Candidate Gene Cloning and Functional Analysis of Genes Involved in VLCFAs Synthesis." *Iowa State University Digital Repository - Retrospective Theses and Dissertations*, Iowa State University, 2007, lib.dr.iastate.edu/rtd/15060.

FAOSTAT, 2018, [www.fao.org/faostat/en/#data/QC](http://www.fao.org/faostat/en/#data/QC).

Fich, Eric A., Nicholas A. Segerson, and Jocelyn K. C. Rose. “The Plant Polyester Cutin: Biosynthesis, Structure, and Biological Roles.” *Annual Review of Plant Biology*, vol. 67, no. 1, 2016, pp. 207–233., doi:10.1146/annurev-arplant-043015-111929.

Flyckt, Kayla S. “Exploring the Genetic Redundancy of *Zea mays* Fatty Acid Elongase (FAE).” *Iowa State University Digital Repository - Retrospective Theses and Dissertations*, Iowa State University, 2016, <https://lib.dr.iastate.edu/etd/15908/>.

Gilbert, R. D., A. M. Johnson, and Ralph A. Dean. “Chemical Signals Responsible for Appressorium Formation in the Rice Blast Fungus *Magnaporthe grisea*.” *Physiological and Molecular Plant Pathology*, vol. 48, no. 5, 1996, pp. 335–346., doi:10.1006/pmpp.1996.0027.

Hansjakob, A., M. Riederer, and Ulrich Hildebrandt. “Wax Matters: Absence of Very-Long-Chain Aldehydes from the Leaf Cuticular Wax of the *glossy11* Mutant of Maize Compromises the Prepenetration Processes of *Blumeria graminis*.” *Plant Pathology*, vol. 60, no. 6, 2011, pp. 1151–1161., doi:10.1111/j.1365-3059.2011.02467.x.

Heller, Jens, and Paul Tudzynski. “Reactive Oxygen Species in Phytopathogenic Fungi: Signaling, Development, and Disease.” *Annual Review of Phytopathology*, vol. 49, no. 1, 2011, pp. 369–390., doi:10.1146/annurev-phyto-072910-095355.

Horbach, Ralf, Aura Rocio Navarro-Quesada, Wolfgang Knogge, and Holger B. Deising. “When and How to Kill a Plant Cell: Infection Strategies of Plant Pathogenic Fungi.” *Journal of Plant Physiology*, vol. 168, no. 1, 2011, pp. 51–62., doi:10.1016/j.jplph.2010.06.014.

Horwitz, Benjamin A., Bradford J. Condon, and B. Gillian Turgeon. “*Cochliobolus heterostrophus*: A Dothideomycete Pathogen of Maize.” *Soil Biology Genomics of Soil- and Plant-Associated Fungi*, 2013, pp. 213–228., doi:10.1007/978-3-642-39339-6\_9.

Hwang, Cheng-Shine, Moshe A. Flaishman, and Pappachan E. Kolattukudy. “Cloning of a Gene Expressed during Appressorium Formation by *Colletotrichum gloeosporioides* and a Marked Decrease in Virulence by Disruption of This Gene.” *The Plant Cell*, vol. 7, no. 2, 1995, p. 183., doi:10.2307/3869994.

Inada, Noriko, and Elizabeth A. Savory. “Inhibition of Prepenetration Processes of the Powdery Mildew *Golovinomyces orontii* on Host Inflorescence Stems Is Reduced in the Arabidopsis Cuticular Mutant *cer3* but Not in *cer1*.” *Journal of General Plant Pathology*, vol. 77, no. 5, 2011, pp. 273–281., doi:10.1007/s10327-011-0331-0.

Javelle, Marie, Vanessa Vernoud, Peter M. Rogowsky, and Gwyneth C. Ingram. “Epidermis: the Formation and Functions of a Fundamental Plant Tissue.” *New Phytologist*, vol. 189, no. 1, 2010, pp. 17–39., doi:10.1111/j.1469-8137.2010.03514.x.

- Jenks, Matthew A., and Edward N. Ashworth. "Plant Epicuticular Waxes: Function, Production, and Genetics." *Horticultural Reviews*, 2010, pp. 1–68., doi:10.1002/9780470650752.ch1.
- Jenks, Matthew A., Sanford D. Eigenbrode, and Bertrand Lemieux. "Cuticular Waxes of *Arabidopsis*." *The Arabidopsis Book*, vol. 1, 2002, doi:10.1199/tab.0016.
- Jenks, Matthew A., Aaron M. Rashotte, Hillary A. Tuttle, and Kenneth A. Feldmann. "Mutants in *Arabidopsis thaliana* Altered in Epicuticular Wax and Leaf Morphology." *Plant Physiology*, vol. 110, no. 2, 1996, pp. 377–385., doi:10.1104/pp.110.2.377.
- Jetter, Reinhard, Ljerka Kunst, and A. Lacey Samuels. "Composition of Plant Cuticular Waxes." *Biology of the Plant Cuticle*, 2006, pp. 145–181., doi:10.1002/9780470988718.ch4.
- Jones, Jonathan D. G., and Jeffery L. Dangl. "The Plant Immune System." *Nature*, vol. 444, no. 7117, 16 Nov. 2006, pp. 323–329., doi:10.1038/nature05286.
- Khan, A., and T. Hsiang. "The Infection Process of *Colletotrichum graminicola* and Relative Aggressiveness on Four Turfgrass Species." *Canadian Journal of Microbiology*, vol. 49, no. 7, 2003, pp. 433–442., doi:10.1139/w03-059.
- Krakowsky, M. D., M. Lee, L. Garay, W. Woodman-Clikeman, M. J. Long, N. Sharapova, B. Frame, and K. Wang. "Quantitative Trait Loci for Callus Initiation and Totipotency in Maize (*Zea Mays* L.)." *Theoretical and Applied Genetics*, vol. 113, no. 5, 2006, pp. 821–830., doi:10.1007/s00122-006-0334-y.
- Lawson, Emily J.R., and R. Scott Poethig. "Shoot Development in Plants: Time for a Change." *Trends in Genetics*, vol. 11, no. 7, 1995, pp. 263–268., doi:10.1016/s0168-9525(00)89072-1.
- Lequeu, José, Marie-Laure Fauconnier, Antoine Chammaï, Roberte Bronner, and Elizabeth Blée. "Formation of Plant Cuticle: Evidence for the Occurrence of the Peroxygenase Pathway." *The Plant Journal*, vol. 36, no. 2, 2003, pp. 155–164., doi:10.1046/j.1365-313x.2003.01865.x.
- Lev, Sophie, Ruthi Hadar, Paolo Amedeo, Scott E. Baker, O. C. Yoder, and Benjamin A. Horwitz. "Activation of an AP1-Like Transcription Factor of the Maize Pathogen *Cochliobolus heterostrophus* in Response to Oxidative Stress and Plant Signals." *Eukaryotic Cell*, vol. 4, no. 2, 2005, pp. 443–454., doi:10.1128/ec.4.2.443-454.2005.
- Li, Fengling, Xuemin Wu, Patricia Lam, David Bird, Huanquan Zheng, Lacey Samuels, Reinhard Jetter, and Ljerka Kunst. "Identification of the Wax Ester Synthase/Acyl-Coenzyme A:Diacylglycerol Acyltransferase WSD1 Required for Stem Wax Ester Biosynthesis in *Arabidopsis*." *Plant Physiology*, vol. 148, no. 1, 2008, pp. 97–107., doi:10.1104/pp.108.123471.

- Li, Li, Delin Li, Sanzhen Liu, Xiaoli Ma, Charles R. Dietrich, Heng-Cheng Hu, Gaisheng Zhang, Zhiyong Liu, Jun Zheng, Guoying Wang, and Patrick S. Schnable. “The Maize *glossy13* Gene, Cloned via BSR-Seq and Seq-Walking Encodes a Putative ABC Transporter Required for the Normal Accumulation of Epicuticular Waxes.” *PLoS ONE*, vol. 8, no. 12, 2013, doi:10.1371/journal.pone.0082333.
- Li, Li, Yicong Du, Cheng He, Charles R. Dietrich, Jiankun Li, Xiaoli Ma, Rui Wang, Qiang Liu, Sanzhen Liu, Guoying Wang, Patrick S. Schnable, and Jun Zheng. “The Maize *glossy6* Gene Is Involved in Cuticular Wax Deposition and Drought Tolerance.” *Journal of Experimental Botany*, 2019, doi:10.1093/jxb/erz131.
- Liu, Sanzhen, Charles R. Dietrich and Patrick S. Schnable. “DLA-Based Strategies for Cloning Insertion Mutants: Cloning the *gl4* Locus of Maize Using *Mu* Transposon Tagged Alleles.” *Genetics*, vol. 183, no. 4, 2009, pp. 1215–1225., doi:10.1534/genetics.109.108936.
- Liu, Sanzhen, Cheng-Ting Yeh, Ho Man Tang, Dan Nettleton, and Patrick S. Schnable. “Gene Mapping via Bulk Segregant RNA-Seq (BSR-Seq).” *PLoS ONE*, vol. 7, no. 5, 2012, doi:10.1371/journal.pone.0036406.
- Maldonado, Ana M., Peter Doerner, Richard A. Dixon, Chris J. Lamb, and Robin K. Cameron. “A Putative Lipid Transfer Protein Involved in Systemic Resistance Signalling in *Arabidopsis*.” *Nature*, vol. 419, no. 6905, 2002, pp. 399–403., doi:10.1038/nature00962.
- Manching, Heather C., Peter J. Balint-Kurti, and Ann E. Stapleton. “Southern Leaf Blight Disease Severity Is Correlated with Decreased Maize Leaf Epiphytic Bacterial Species Richness and the Phyllosphere Bacterial Diversity Decline Is Enhanced by Nitrogen Fertilization.” *Frontiers in Plant Science*, vol. 5, 15 Aug. 2014, doi:10.3389/fpls.2014.00403.
- McFarlane, Heather E., John J. H. Shin, David A. Bird, and A. Lacey Samuels. “Arabidopsis ABCG Transporters, Which Are Required for Export of Diverse Cuticular Lipids, Dimerize in Different Combinations.” *The Plant Cell*, vol. 22, no. 9, 2010, pp. 3066–3075., doi:10.1105/tpc.110.077974.
- Mendgen, K., Hahn, M., Deising, H. “Morphogenesis and Mechanisms of Penetration by Plant Pathogenic Fungi.” *Annual Review of Phytopathology*, vol. 34, no. 1, 1996, pp. 367–386., doi:10.1146/annurev.phyto.34.1.367.
- Mercure, E. W., Hitoshi Kunoh, and Ralph L. Nicholson. “Adhesion of *Colletotrichum graminicola* Conidia to Corn Leaves, a Requirement for Disease Development.” *Physiological and Molecular Plant Pathology*, vol. 45, no. 6, 1994, pp. 407–420., doi:10.1016/s0885-5765(05)80039-6.

- Moose, Stephen P, and Paul H. Sisco. “*Glossy15*, An *APETALA2*-like Gene from Maize That Regulates Leaf Epidermal Cell Identity.” *Genes & Development*, vol. 10, no. 23, 1996, pp. 3018–3027., doi:10.1101/gad.10.23.3018.
- Neuffer, M. Gerald, Edward H. Coe, and Susan R. Wessler. *Mutants of Maize*. Cold Spring Harbor Laboratory Press, 1997.
- O'Connell, Richard J., Michael R. Thon, Stéphane Hacquard, Stefan G. Amyotte, Jochen Kleemann, Maria F. Torres, Ulrike Damm, Ester A. Buiate, Lynn Epstein, Noam Alkan, Janine Altmüller, Lucia Alvarado-Balderrama, Christopher A. Bauser, Christian Becker, Bruce W. Birren, Zehua Chen, Jaeyoung Choi, Jo Anne Crouch, Jonathan P. Duvick, Mark A. Farman, Pamela Gan, David Heiman, Bernard Henrissat, Richard J. Howard, Mehdi Kabbage, Christian Koch, Barbara Kracher, Yasuyuki Kubo, Audrey D. Law, Marc-Henri Lebrun, Yong-Hwan Lee, Itay Miyara, Neil Moore, Ulla Neumann, Karl Nordström, Daniel G. Panaccione, Ralph Panstruga, Michael Place, Robert H. Proctor, Dov Prusky, Gabriel Rech, Richard Reinhardt, Jeffrey A. Rollins, Steve Rounsley, Christopher L. Schardl, David C. Schwartz, Narmada Shenoy, Ken Shirasu, Usha R. Sikhakolli, Kurt Stüber, Serenella A. Sukno, James A. Sweigard, Yoshitaka Takano, Hiroyuki Takahara, Frances Trail, H. Charlotte van der Does, Lars M. Voll, Isa Will, Sara Young, Qiandong Zeng, Jingze Zhang, Shiguo Zhou, Martin B. Dickman, Paul Schulze-Lefert, Emiel Ver Loren van Themaat, Li-Jun Ma, and Lisa J. Vaillancourt. “Lifestyle Transitions in Plant Pathogenic *Colletotrichum* Fungi Deciphered by Genome and Transcriptome Analyses.” *Nature Genetics*, vol. 44, no. 9, 2012, pp. 1060–1065., doi:10.1038/ng.2372.
- Pascholati, Sergio F., Holger Bruno Deising, B. Leiti, Donald W. Anderson, and Ralph L. Nicholson. “Cutinase and Non-Specific Esterase Activities in the Conidial Mucilage of *Colletotrichum graminicola*.” *Physiological and Molecular Plant Pathology*, vol. 42, no. 1, 1993, pp. 37–51., doi:10.1006/pmpp.1993.1004.
- Pfeilmeier, Sebastian, Delphine L. Caly, and Jacob G. Malone. “Bacterial Pathogenesis of Plants: Future Challenges from a Microbial Perspective.” *Molecular Plant Pathology*, vol. 17, no. 8, 2016, pp. 1298–1313., doi:10.1111/mpp.12427.
- Reina-Pinto, José J., Derry Voisin, Sergey Kurdyukov, Andrea Faust, Richard P. Haslam, Louise V. Michaelson, Nadia Efremova, Benni Franke, Lukas Schreiber, Johnathan A. Napier, and Alexander Yephremov. “Misexpression of FATTY ACID ELONGATION1 in the Arabidopsis Epidermis Induces Cell Death and Suggests a Critical Role for Phospholipase A2 in This Process.” *The Plant Cell Online*, vol. 21, no. 4, 2009, pp. 1252–1272., doi:10.1105/tpc.109.065565.
- Schall, R. A., Ralph L. Nicholson, and H. L. Warren. “Influence of Light on Maize Anthracnose in the Greenhouse.” *Phytopathology*, vol. 70, no. 10, 1980, p. 1023., doi:10.1094/phyto-70-1023.

- Schweizer, Patrick, A. Jeanguenat, D. Whitacre, Jean Pierre Métraux, and Egon M. Möisinger. “Induction of Resistance in Barley Against *Erysiphe graminis* f.sp. *hordei* by Free Cutin Monomers.” *Physiological and Molecular Plant Pathology*, vol. 49, no. 2, 1996, pp. 103–120., doi:10.1006/pmpp.1996.0043.
- Sekhon, Rajandeep S., Haining Lin, Kevin L. Childs, Candice N. Hansey, C. Robin Buell, Natalia de Leon, and Shawn M. Kaeppler. “Genome-Wide Atlas of Transcription during Maize Development.” *The Plant Journal*, vol. 66, no. 4, 2011, pp. 553–563., doi:10.1111/j.1365-313x.2011.04527.x.
- Shumborski, Sarah J., A. Lacey Samuels, and David A. Bird. “Fine Structure of the Arabidopsis Stem Cuticle: Effects of Fixation and Changes over Development.” *Planta*, vol. 244, no. 4, 2016, pp. 843–851., doi:10.1007/s00425-016-2549-8.
- “Southern Leaf Blight.” *Southern Leaf Blight*, DuPont Pioneer, 2010, [www.pioneer.com/home/site/us/agronomy/crop-management/corn-insect-disease/southern-leaf-blight/](http://www.pioneer.com/home/site/us/agronomy/crop-management/corn-insect-disease/southern-leaf-blight/).
- Stelplflug, Scott C., Rajandeep S. Sekhon, Brieanne Vaillancourt, Candice N. Hirsch, C. Robin Buell, Natalia de Leon, and Shawn M. Kaeppler. “An Expanded Maize Gene Expression Atlas Based on RNA Sequencing and Its Use to Explore Root Development.” *The Plant Genome*, vol. 9, no. 1, Mar. 2016, doi:10.3835/plantgenome2015.04.0025.
- Sturaro, Monica, Hans Hartings, Elmon Schmelzer, Riccardo Velasco, Francesco Salamini, and Mario Motto. “Cloning and Characterization of *GLOSSY1*, a Maize Gene Involved in Cuticle Membrane and Wax Production.” *Plant Physiology*, vol. 138, no. 1, 2005, pp. 478–489., doi:10.1104/pp.104.058164.
- Tacke, Eckhard, Christian Korfhage, Delef Michel, Massimo Maddaloni, Mario Motto, Simona Lanzini, Francesco Salamini, and Hans-Peter Döring. “Transposon Tagging of the Maize *glossy2* Locus with the Transposable Element *En/Spm*.” *The Plant Journal*, vol. 8, no. 6, 1995, pp. 907–917., doi:10.1046/j.1365-313x.1995.8060907.x.
- Ullstrup, A J. “The Impacts of the Southern Corn Leaf Blight Epidemics of 1970-1971.” *Annual Review of Phytopathology*, vol. 10, no. 1, 1972, pp. 37–50., doi:10.1146/annurev.py.10.090172.000345.
- Venard, Claire Marie-Pierre. “The Development of *Colletotrichum graminicola* Inside Maize Stalk Tissues.” *University of Kentucky Doctoral Dissertations, University of Kentucky*, 2006, [uknowledge.uky.edu/gradschool\\_diss/439](http://uknowledge.uky.edu/gradschool_diss/439).
- Warren, H.L., *et al.* “Observations of *Colletotrichum graminicola* in Indiana.” *Plant Disease Reporter*, vol. 57, 1973, pp. 143–144.
- Weihmann, Fabian, Iris Eisermann, Rayko Becher, Jorrit-Jan Krijger, Konstantin Hübner, Holser B. Deising, and Stefan G. R. Wirsal. “Correspondence between Symptom Development

- of *Colletotrichum graminicola* and Fungal Biomass, Quantified by a Newly Developed qPCR Assay, Depends on the Maize Variety.” *BMC Microbiology*, vol. 16, no. 1, 23 May 2016, doi:10.1186/s12866-016-0709-4.
- Wu, Dongliang, Shinichi Oide, Ning Zhang, May Yee Choi, and B. Gillian Turgeon. “ChLae1 and ChVel1 Regulate T-Toxin Production, Virulence, Oxidative Stress Response, and Development of the Maize Pathogen *Cochliobolus heterostrophus*.” *PLoS Pathogens*, vol. 8, no. 2, 2012, doi:10.1371/journal.ppat.1002542.
- Xia, Ye, Qing-Ming Gao, Keshun Yu, Ludmila Lapchyk, DuRoy Navarre, David Hildebrand, Aardra Kachroo, and Pradeep Kachroo. “An Intact Cuticle in Distal Tissues is Essential for the Induction of Systemic Acquired Resistance in Plants.” *Cell Host & Microbe*, vol. 5, no. 2, 2009, pp. 151–165., doi:10.1016/j.chom.2009.01.001.
- Xu, Xiaojie, Charles R. Dietrich, Rene Lessire, Basil J. Nikolau, and Patrick S. Schnable. “The Endoplasmic Reticulum-Associated Maize GL8 Protein is a Component of the Acyl-Coenzyme A Elongase Involved in the Production of Cuticular Waxes.” *Plant Physiology*, vol. 128, no. 3, 2002, pp. 924–934., doi:10.1104/pp.010621.
- Yeats, Trevor H., and Jocelyn K. C. Rose. “The Formation and Function of Plant Cuticles.” *Plant Physiology*, vol. 163, no. 1, 2013, pp. 5–20., doi:10.1104/pp.113.222737.
- Zabka, Vanessa, Michaela Stangl, Gerhard Bringmann, Gerd Vogg, Markus Riederer, and Ulrich Hildebrandt. “Host Surface Properties Affect Prepenetration Processes in the Barley Powdery Mildew Fungus.” *New Phytologist*, 2007, doi:10.1111/j.1469-8137.2007.02233.x.
- Zacchino, Susana A., Estefania Butassi, Melina Di Liberto, Marcela Raimondi, Agustina Postigo, and Maximiliano Sortino. “Plant Phenolics and Terpenoids as Adjuvants of Antibacterial and Antifungal Drugs.” *Phytomedicine*, vol. 37, 2017, pp. 27–48., doi:10.1016/j.phymed.2017.10.018.
- Zheng, Huanquan, Owen Roland, and Ljerka Kunst. “Disruptions of the Arabidopsis Enoyl-CoA Reductase Gene Reveal an Essential Role for Very-Long-Chain Fatty Acid Synthesis in Cell Expansion during Plant Morphogenesis.” *The Plant Cell Online*, vol. 17, no. 5, 2005, pp. 1467–1481., doi:10.1105/tpc.104.030155.
- Zheng, Jun, Cheng He, Yang Qin, Guifang Lin, Woojun D. Park, Minghao Sun, Jian Li, Xiaoduo Lu, Chunyi Zhang, Cheng-Ting Yeh, Chathura J. Gunasekara, Erliang Zeng, Hairong Wei, Patrick S. Schnable, Guoying Wang, and Sanzhen Liu. “Co-Expression Analysis Aids in the Identification of Genes in the Cuticular Wax Pathway in Maize.” *The Plant Journal*, 2018, doi:10.1111/tpj.14140.

Ziv, Carmit, Zhenzhen Zha, Yu G. Gao, and Ye Xia. “Multifunctional Role of Plant Cuticle during Plant-Pathogen Interactions.” *Frontiers in Plant Science*, vol. 9, 2018, doi:10.3389/fpls.2018.01088.